이학 석사 학위논문

Highly Stable Rhodium Nanoparticles Functionalized by Vinylidene Group:

Synthesis, Surface Reaction, and Catalysis

Vinylidene기로 활성화된 안정한 로듐 나노입자:

합성, 표면에서의 반응, 그리고 촉매 반응

2015년 8월

서울대학교 대학원

화학부 유기화학

박 상 승

Highly Stable Rhodium Nanoparticles Functionalized by Vinylidene Group: Synthesis, Surface Reaction, and Catalysis

Vinylidene기로 활성화된 안정한 로듐 나노입자: 합성, 표면에서의 반응, 그리고 촉매 반응

지도교수 Soon Hyeok Hong
이 논문을 이학석사학위논문으로 제출함
2015년 6월
서울대학교 대학원

화학부 유기화학
박 상 승
박상승의 석사학위논문을 인준함

2015년 8월

위 원 장 이 철 범 (인)
부 위 원 장 Soon Hyeok Hong(인)
위 원 정 영 근 (인)

Abstract

Highly Stable Rhodium Nanoparticles Functionalized by Vinylidene Group: Synthesis, Surface Reaction, and Catalysis

Sangseung Park

Chemistry Department, Organic Chemistry

The Graduate Schol

Seoul National University

Covalent functionalization of nanomaterials in the catalysis have been fascinated by many researchers as one of the solutions to the problems evoked by prohibiting the unnecessary interaction between the catalysts during the reactions. Above all, we focused on the vinylidene ligand, which had been resulted in transformation to other carbon-based ligands which had not been released from the metal fragment in homogeneous catalysis, for the development with catalytic applications of the nanomaterials. In this paper, we successfully synthesized vinylidene functionalized rhodium nanoparticles and characterized them

using several tools. Especially, for the confirmation of the vinylidene group on the surface, we showed the NMR study, and surface reaction. After the characterization, we applied the vinylidene functionalized rhodium nanoparticles to the hydroformylation reaction. In the catalytic application, we showed that the rhodium nanoparticles had the excellent activity in the hydroformylation reaction and the nanoparticles is more stable than the nanoparticle using other surfactant or ligand by recycle test. And also, we showed the difference of the catalytic activity according to the vinylidene species.

Keyword : functionalization by vinylidene; rhodium nanoparticle; surface reaction; catalytic application; stability

KeywordStudent Number : 2012-23044

Table of Contents

List of Figures

List of Tables

List of Schemes

Introduction

Since 1990s, nanoparticles have been to the fore by the material scientists due to unusual properties and the synthetic method of nanoparticles has been developed using various ligand, like amine, phosphate, thiol and carboxylic acid, because the size, shape, morphology and surface properties of the nanoparticles could be changed according to the ligand[1]. Relatively recently, covalent functionalization of nanomaterials has been fascinated by many researchers because it gives an opportunity to tune the electronic and optical properties by simply modifying the surface without changing the core[2]. As a considerable numbers of studies have been conducted on the covalent functionalization of carbon-based materials[2], the interest on the covalent functionalization of inorganic nanomaterials has been tremendously increased[3]. In the catalysis field, many research group proposed the covalent fixation of catalyst on the surface of inorganic nanomaterials to utilize their high surface area[4]. By forming the rigid bond between the catalyst and inorganic support, the activity and stability of catalyst was secured by prohibiting the unnecessary interaction between the catalysts during the reaction[5]. In case of using the inorganic core as a

catalyst, however, only few reports were made regarding the covalent functionalization. Recently, The S. Chen group reported the synthesis of vinylidene functionalized Ru nanoparticles[6] and demonstrated that the metal-vinylidene bond formation could be easily achieved by introducing the alkyne derivatives during ligand exchange process. Inspired by this work, we adopted the mechanism of vinylidene functionalization to synthesize vinylidene functionalized Rh nanoparticles, which is known as an intimate counterpart of rutheniumin catalysis, and successfully utilized as a hydrformylation reaction catalyst.

From the best of our knowledge, this is the first report using vinylidene functionalized Rh nanoparticle using as a catalyst. Furthermore, the synthesized nanoparticles showed high stability through the multiple recycled reactions, which is contrast to the previously reported carbene functionalized nanoparticles[7].

Results and discussion

We successfully synthesized vinylidene functionalized Rh nanoparticles via 1,2-propandiol reduction, followed by ligand exchange process (the detailed synthetic procedures are described in the supporting information). In typical synthesis, rhodium(III) chloride hydrate, sodium acetate trihydrate and 1,2-propanediol were stirred gently for 30 min at room temperature. The temperature of mixture solution was increased until it reaches to 165 °C, and kept at this temperature for 2hr. At this point, the color of mixture solution turned complete black from transparent yellow, which indicates the rhodium nanoparticles were formed with the help of 1,2-propandiol and the sufficiently high temperature. After the reaction termination, the mixture solution was cooled down to room temperature and rinsed excessively with the mixture of methanol and ethanol. To attach vinylidene ligand on the surface of Rh nanoparticles, acetylene terminated ligands were introduced to the nanoparticles dispersed in toluene at the ratio of 1mmol ligand per 1mg of nanoparticles (typically, we used phenylacetylene for the model reactions). This procedure leads to the formation of intermediate η^2-alkyne complex on the Rh nanoparticle surface, which result in rearrangement to the η

[1]-vinylidene via 1,3-H shifts[8]. The reaction mixture was kept at room temperature for overnight with vigorous stirring. The resulting products were rinsed again with methanol and ethanol to remove residual unreacted organic ligands. After the washing process, vinylidene functionalized Rh nanoparticles were dried at the vacuum oven for an hour.

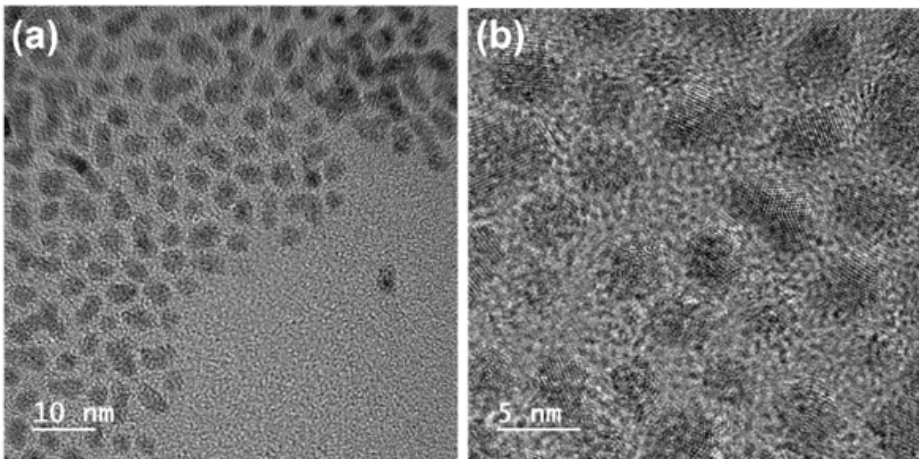

Figure 1. TEM images of vinylidene functionalized Rh nanoparticles.

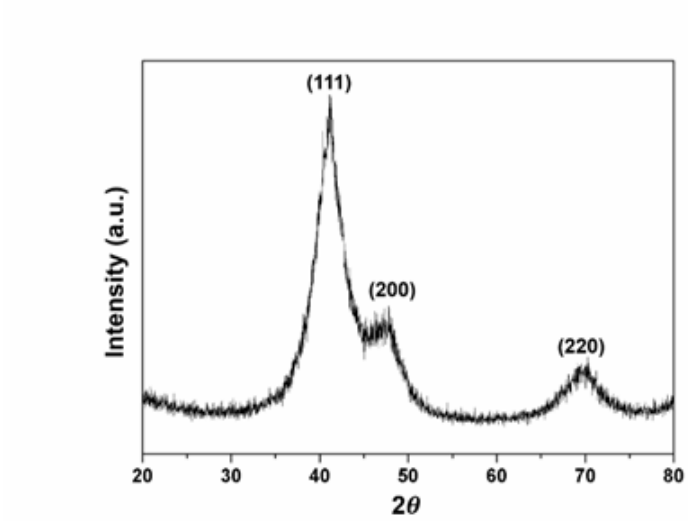

Figure 2. The powder X-ray diffraction (XRD) pattern of the synthesized catalyst (PDF#: 05-0685).

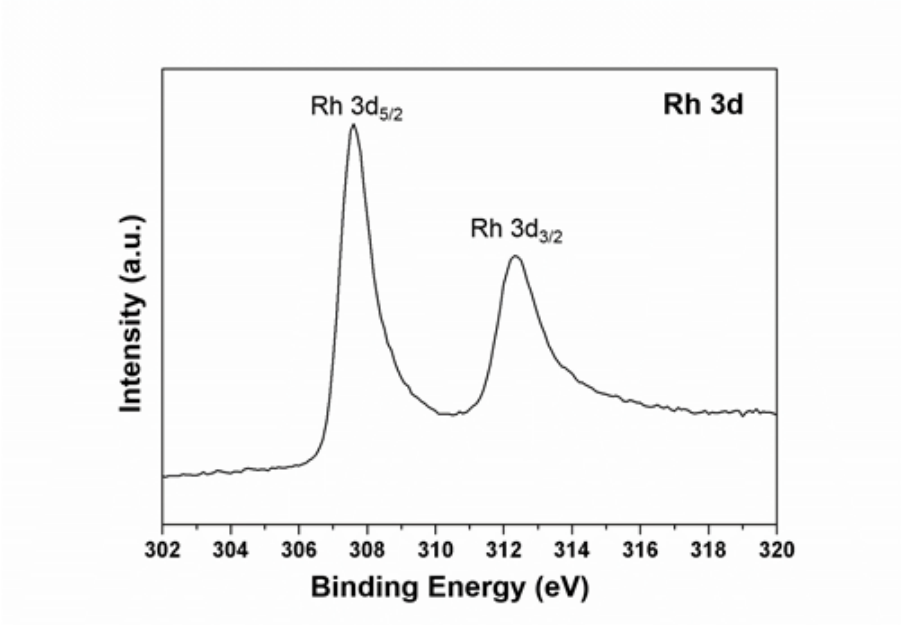

Figure 3. Rh 3d X-Ray photoelectron spectra of the vinylidene functionalized Rh nanoparticles.

Transmission electron microscope (TEM) images of the synthesized nanoparticles reveal that the size range of nanoparticles were 3 to 4 nm (Figure 1), and the powder X-ray diffraction (XRD) pattern shows that the oxidation state of the nanoparticles is Rh^0 (Figure 2). Since catalytic reaction only occurs on the surface of heterogeneous catalyst, we confirmed that the surface of synthesized Rh nanoparticles were also close to Rh^0 from X-ray photoelectron spectra (Figure 3). The Rh 3d spectra indicates (the binding energy of Rh 3d5/2 at 307.5 and Rh 3d3/2 at 312.3) that the surface of as-synthesized Rh

nanoparticles were Rh^0 (the binding energy of Rh 3d5/2 at 307.3 and Rh 3d3/2 at 312.0) while binding energies of Rh2O3 has 308.4 at Rh 3d5/2 and 313.3 at Rh 3d3/2. The partial oxidation of Rh nanoparticles, leading peaks shift to the higher binding energies, was inevitable due to the size effect, which is previously reported phenomena[9].

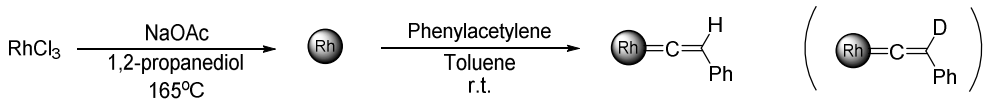

Scheme 1. Synthesis of vinylidene functionalized rhodium nanoparticles with phenylacetylene-D.

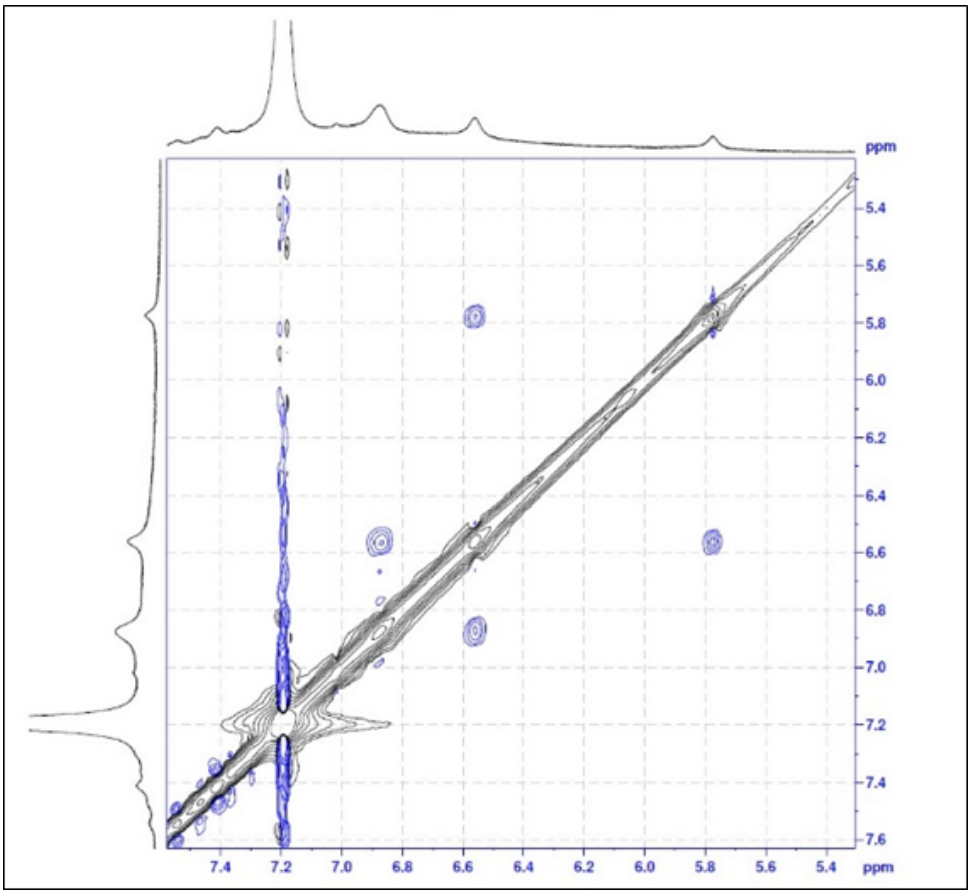

Figure 4. The rotating frame overhause effect spectroscopy of the Rh nanoparticles.

Due to the peak broadening of 1H proton NMR, the peaks could not be exactly assigned. This is a generally observed phenomenon in the NMR spectra of ligands tightly bound on the surface of nanoparticles[10] (Figure S2a). Thus, we performed rotating frame overhause effect spectroscopy (ROESY) NMR analysis to verify the existence of the vinylidene group on the

surface of Rh nanoparticles. Generally, the NMR peak of the proton, which is located on the vinylidene group, is existed at 4 to 0 ppm in 1H-NMR spectroscopy and the peak was shifted to down-field as rhodium metal is more electron-rich[11]. The ROESY NMR data showed that the proton of vinylidene group, the peak at 5.85 ppm, was strongly interacting with the protons of phenyl rings. To confirm that the peak at 5.85 ppm correspond to the proton of vinylidene group, we performed the ligand exchange process with the deuterium substituted phenylacetylene (phenylacetylene-D, Scheme 1). As expected, the intensity of peak at 5.85 ppm was decreased while the other phenyl ring peaks showed unchanged. As a result, we concluded that the peak at 5.85 ppm correspond to the proton of vinylidene group. This vinylidene proton peak could be shifted to upfield or downfield depending on the electron-richness of phenyl ring. When fluorine group or methyl group was located on the para position, the vinylidene proton was shifted to upfield (5.75 ppm or 5.81 ppm) (Table S1). However, the peak of vinylidene proton was shifted to downfield (6.17 ppm) in the case of 4-methoxy phenylacetylene, which indicates that position of vinylidene proton peak was strongly affected by the electron-richness of phenyl ring.

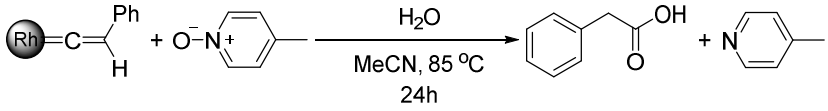

Scheme 2. C-O oxidation reaction.

Further, we performed an oxgenative addition reaction on surface to check if vinylidene groups are properly functionalized on the Rh nanoparticle surface (Scheme 2). In a recent study, the C. Lee group demonstrated rhodium-catalyzed oxygenative addition reaction to terminal alkynes, which involves formation of a rhodium vinylidene complex, for the synthesis of carboxylic acids[12]. Mechanistically, η^1-isomer of the π-alkyne rhodium complex is essential to yield ketene from the oxygenation of vinylidene complex (Figure 5). We used 4-picoline N-oxide as an oxygen donor and water as a nucleophile to confirm the identity of vinylidene functionalization conclusively, with a fundamental question of whether such reaction can take place on the surface of nanoparticles. To our delight, we observed phenylacetic acid from the oxygenative addition reaction on surface, signifying vinylidene groups were successfully functionalized on the surface of Rh nanoparticles. To quantify the yield (90 %) of the reaction, we got the CHNS data of Rh nanoparticles and compared to the result of the oxygenative addition reaction. Using this method, we could quantify the amount of vinylidene functionalization on Rh nanoparticles. Thus,

we concluded that the Rh nanoparticles were successfully functionalized with the vinylidene group.

Since the hydroformylation reaction was discovered by Otto Roelen in 1938, this reaction is the largest homogeneous catalytic process in industry, which produce more 15 billion pounds of aldehydes or alcohols per year, and, although the process was well developed since 1938, many researchers have been interested in hydroformylation reaction for the improvement of the selectivity to linear or branched products and the activity in mild conditions[13]. Vinylidene functionalized Rh nanoparticle showed excellent activity towards hydroformylation reaction starting with various substrates (Table 1). For the styrene derivatives, para-substituted compounds were successfully converted to the corresponding products regardless of electron-donating or -withdrawing groups with branched form aldehyde as a major product. Interestingly, CF_3 substituted styrene showed the highest regioselectivity while the other electron withdrawing group, chlorine, substituted styrene showed the similar regioselectivity with the model reaction. Unfortunately, our rhodium nanoparticle was not active for the hydroformylation of internal olefin, but terminal aliphatic compound showed complete conversion of reaction product with the linear-formed aldehyde as a major product.

TABLE 1. Substrate scope of hydroformylation reaction[a]

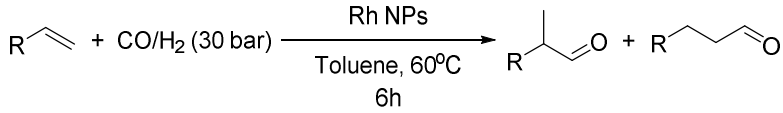

Entry	Substrate	Conversion (%)[b]	Selectivity (*b:l*)[b]
1	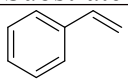	100[c]	84.3 : 15.7
2	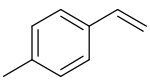	82	74.9 : 25.1
3	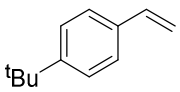	100	79.1 : 20.9
4	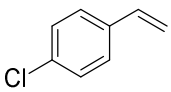	100	75.2 : 24.8
5	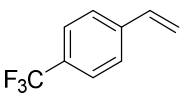	83	97.0 : 3.0
6	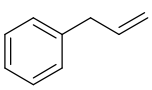	100	30.0 : 70.0
7	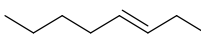	0	-

[a] Hydroformylation condition: olefin (10 mmol), Rh nanoparticles (10.2 mg), toluene (10 ml), CO (initial pressure, 15 bar), H_2 (initial pressure, 15 bar), reaction temperature (60°C), and reaction time (6 h). [b] Conversion and selectivity were determined by ^{1}H NMR. [c] Conversion and selectivity in entry 1 were determined by gas chromatography using dodecane as an internal standard.

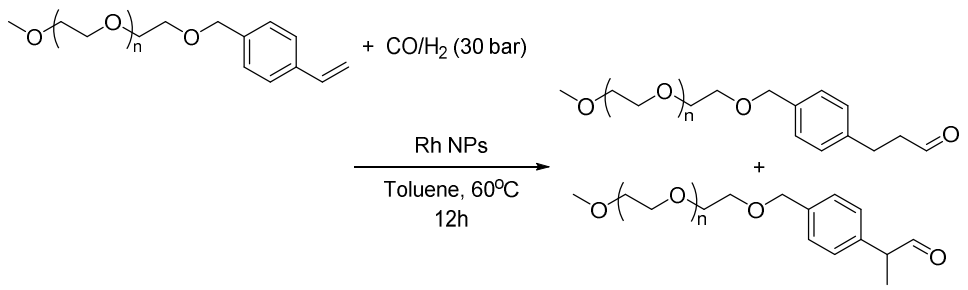

Scheme 3. Three phase reaction.

To show this is a complete heterogeneous reaction, we performed designed reaction called 'three phase reaction' (Scheme 3)[14]. Basic idea of the study is to know if this reaction is going with leached out metal moiety or fully running with the heterogeneous nanoparticles by comparing the reaction completion time, using two different types of substrates. One reaction starts with a substrate attached to the insoluble support while the other reaction starts with an analogous soluble substrate. If the reaction only proceeds with the heterogeneous catalyst, the supported substrate will react much slower than the freestanding soluble substrate. Conversely, there will be no difference in the completion time between the designed reactions, in case of leached out catalyst plays a major role to complete the reaction. We immobilized styrene to (Polyethyleneglycol)-methyl ether and used as an insoluble supported substrate. As expected, it took more than 2 days to complete the reaction while it required only

6 hr to complete the reaction with an analogous soluble substrate. Thus, we concluded that the reaction was running under the heterogeneous nanoparticle surface, and there is no leaching effect.

It is well known that the commonly reported nanocatalysts immediately aggregate after the chemical reactions due to the weak binding of ligand on the nanoparticle surface. However, phenylacetylene functionalized Rh nanoparticle showed excellent dispersion after the hydroformylation reaction, while phenylacetic acid and acetate functionalized Rh nanoparticles precipitated even after the long time sonication as shown in Figure 5a. Thanks to the rigid covalent bond formation of organic ligand on the nanoparticle surface, dispersibility of the nanoparticle maintained through the multiple recycling process with high conversion and selectivity (Table 2). After the reaction, no significant particle aggregation or morphology transformation was observed (Figure 5b) and there was similar pattern of Rh 3d X-Ray photoelectron spectra of the vinylidene functionalized Rh nanoparticles (Figure 5C). And also, using 1H-NMR spectroscopy, we confirmed that the vinylidene proton was remained at the hydroformylation reaction condition. We also tested oleic acid, frequently used surfactant in the nanoparticle synthesis, passivated Rh nanoparticles, and it also gave us high conversion and selectivity

at the initial trial. However, activity of the catalyst rapidly dropped after the 2nd or 3rd trial, and it became permanently inactive before 5th recycle.

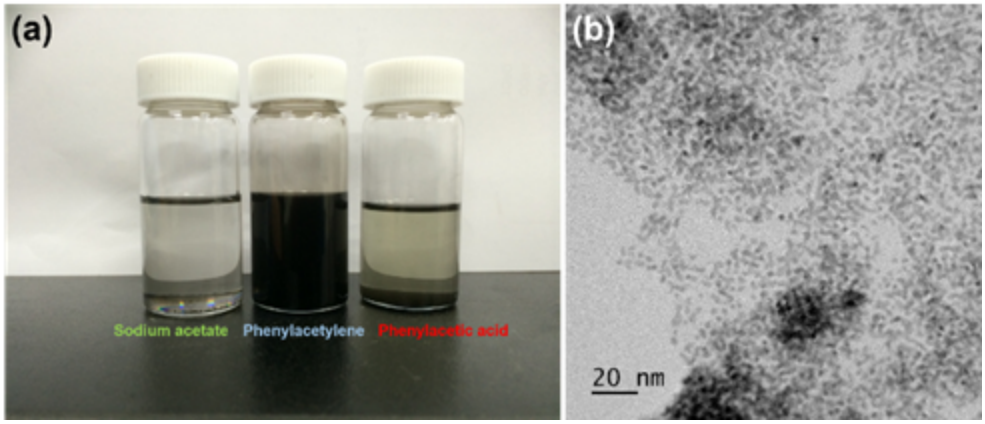

Figure 5. (a) Picture of the catalyst dispersed in the substrate mixture solution before the 2nd recycle. (b) TEM image of the phenylacetylene functionalized Rh nanoparticles after the 1st reaction termination.

Table 2. Recycling results of the phenylacetylene, phenylacetic acid and oleic acid passivated Rh nanocatalysts[a]

Recycle #	Ligand					
	Phenylacetylene		Phenylacetic acid		Oleic acid	
	Conv. (%)	Sel. (b/l)	Conv. (%)	Sel. (b/l)	Conv. (%)	Sel. (b/l)
1	100	5.4	61	4.6	92	6.9
2	100	5.2	45	9.1	87	8.4
3	100	5.6	23	20.3	47	13.7
6	99	5.5				
8	96	6.2				

[a] Conditions: styrene (1.15 ml, 10 mmol), Rh nanoparticles (10.2 mg), toluene (10 ml), CO (initial pressure, 15 bar), H_2 (initial pressure, 15 bar), reaction temperature (60°C), reaction time (6 h), and conversion and selectivity were determined by gas chromatography using dodecane as an internal standard.

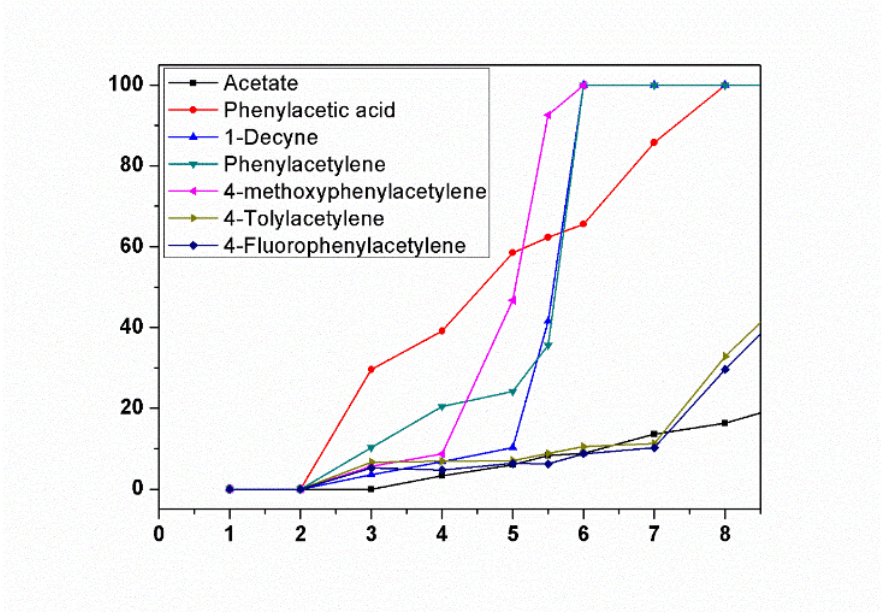

Figure 6. Time-dependent product yield of the hydroformylation reaction using Rh nanoparticles passivated with various ligands.

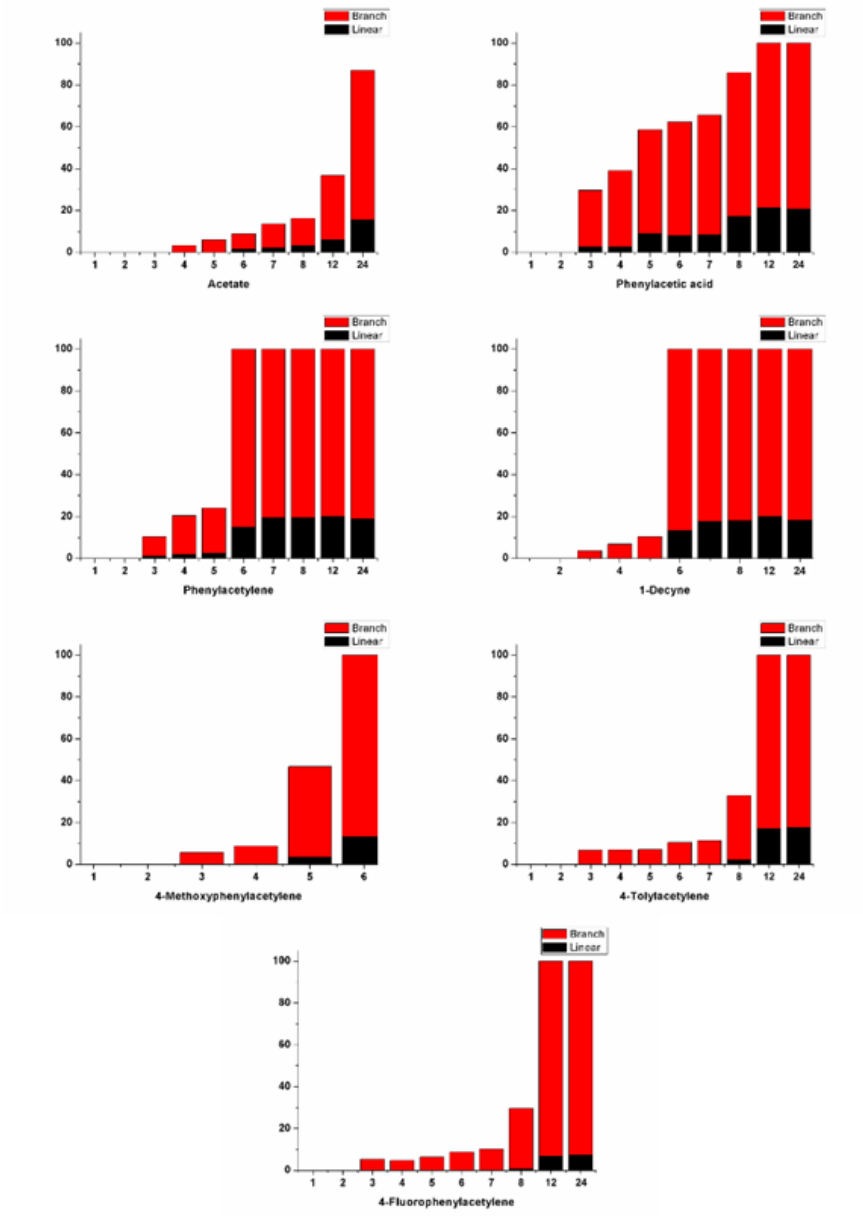

Figure 7. Time-dependent product yield and selectivity of the hydroformylation reaction using Rh nanoparticles passivated with various ligands. (X-axis: conversion, Y-axis: time (h))

By varying the passivating ligand on the surface of Rh nanoparticles via ligand exchange process, it was able to control the reaction kinetics of hydroformylation reaction. To obtain the reaction kinetics profile, we ran the hydroformylation reactions with various vinylidene or carboxylate ligands passivated Rh nanoparticles under identical conditions. During the reaction, aliquots were drawn from the reaction mixtures at an hour interval, and the results are shown on Figure 6 and Figure 7. From the reaction profile, at least three aspects were observed. First, vinylidene functionalized Rh nanoparticle involved hydroformylation reaction required induction time before the rapid conversion of reaction product while carboxylate functionalized ones showed the steady increase of reaction product. Secondly, only branched form was produced at the early stage of the reaction, before it reaches 20% conversion. Ratio of the linear product increase as the reaction proceeds, but never exceeded a certain level. Lastly, each of vinylidene ligand passivated Rh nanoparticles showed different activities. Even though para-substituted phenylacetylene with methyl or fluoro group elongated reaction time, 4-methoxyphenylacetylene passivated Rh nanoparticle accelerated reaction time. The correlativity of the results are under investigation.

Conclusion

In conclusion, we successfully synthesized vinylidene functionalized rhodium nanoparticle and analyze the nanoparticle through the several tools. In the analysis process, it is the first trial of using chemical reaction for characterizing the structure between vinylidene ligand and surface of the nanoparticle. This vinylidene functionalized Rh nanoparicle showed the excellent catalytic activity for the hydroformylation reaction of styrene. As far as we know, this is also the first example of the catalytic reaction using vinylidene functionalized nanoparticles and that showed the difference of the catalytic activity according to the vinylidene species. In the stabilization issue, we found that the vinylidene functionalized rhodium nanoparticle is more stable than the nanoparticle using other surfactant or ligand and could be recycled for catalytic reaction. Based on these results, we suggest that this type of nanoparticle could be prepared using other vinylidene ligand and improve the catalytic activity for the other catalytic system.

Experimental section

Synthesis of vinylidene functionalized Rh nanopar-itcles

In typical synthesis, 100 mg of rhodium(III) chloride hydrate, 220 mg of sodium acetate trihydrate and 140 mL of 1,2-propanediol were stirred gently for 30 min at room temperature. The temperature of mixture solution was increased at the rate of 5 °C per minute until it reaches to 165 °C, and kept at this temperature for 2 hr. After the reaction termination, the mixture solution was cooled down to room temperature and rinsed excessively with mixture of methanol and ethanol. To attach vinylidene ligand on the surface of Rh nanoparticles, acetylene terminated ligands were introduced to the nanoparticles dispersed in 10 mL of toluene at the ratio of 1 mmol ligand per 1 mg of nanoparticles. The reaction mixture was kept at room temperature for overnight with vigorous stirring. The resulting products were rinsed again with methanol and ethanol to remove residual unreacted organic ligands. After the washing process, vinylidene functionalized Rh nanoparticles were dried at the vacuum oven for an hour.

Characterization of rhodium nanoparticles function-

alized with phenylacetylene through rhodium-catalyzed oxygenative addition

20 mg of rhodium nanoaparticles, 131 mg of 4-picoline *N*-oxide, 0.18 mL of water and 0.5 mL of CH_3CN were placed in vial and gently stirred for a minute. The mixture was heated to 60°C and maintained at this temperature for 24 hr. After the reaction, the mixture was filtered for the separation of nanoparticles and the products were analyzed by GC-MS using HP-5 MS column. Dodecane was used as an internal standard. For the ligand amount quantification, vinylidene functionalized Rh nanoparticles were ionized in aqua regia, then toluene was introduced to gather the organic moieties from Rh nanoparticle ionization. Upper organic mixture part was transferred to separate vial and excessively washed with water to remove any acetate ligand or residual acid protons.

General procedure of hydroformylation with Rhodium nanoparticles

10.2 mg of rhodium nanoparticles were dispersed in 10 mL of toluene, and the mixture solution was placed on the high pressure reactor with 1.15 mL of styrene. The solution was purged with CO gas for 10 min. Then, the pressure of the reactor was increased up to 30 atm that consist of 15 atm of

CO gas and 15 atm of H_2 gas. The temperature of reactor was increased until it reaches 60 °C, and maintained at this temperature for 6 hr. After the reaction, the nanoparticles were filtered by celite. The product was analyzed by GC-MS using identical column used in the oxygenative addition reaction analysis. Dodecane was used as a internal standard.

Synthesis of MeOPEG-styrene

2.93 g of (Polyethyleneglycol)-methyl ether (MW : 5000), 0.33g of sodium hydride and 5 mL of dry THF were added to a three-necked flask. The mixture was stirred under an Ar atmosphere for 1 hr. A solution consists of 0.60 g of 4-vinylbenzyl chloride and 5 mL of dry THF was added dropwise to the mixture solution and refluxed at 65 °C overnight[15]. To quench the reaction, reaction batch was cooled down to ambient temperature followed by addition of a few drops of water. THF was removed in vacuo, and 100 mL of dichloromethane was added to dissolve the product. CH_2Cl_2 solution was passed through a pad of celite. After the evaporation of volatiles, the crude mixture was eluted through a pad of silica gel using dichloromethane and methanol, and the product was precipitated from dichloromethane into diethyl ether. The precipitates were collected by a centrifuge to yield a fluffy

white solid[16].

General procedure of Three-Phase Test

500 mg of MeOPEG-styrene and rhodium nanoparticles (1 mol%) were mixed in 10 mL of toluene. Using high pressure reactor, the solution was purged with CO gas for 10 min. Then, the reactor pressure was elevated to 30 atm by injecting 15 atm of CO gas and 15 atm of H_2 gas. The reactor was heated at 60 ℃ and maintained at the given reaction time. After the reaction termination, the nanoparticles were filtered by celite. The solvent was dried in vacuo, and the product was analyzed by ^{1}H-NMR.

Supporting Information

Table S1. Comparison of Chemical Shift of the Vinylidene-proton according to para-substituted phenylacetylene.

	δ H (ppm)[a]
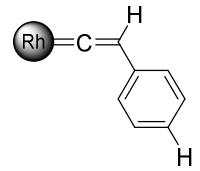	5.87
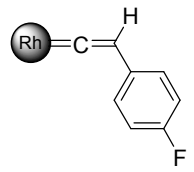	5.75
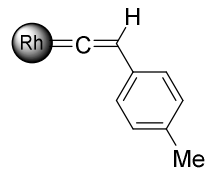	5.81
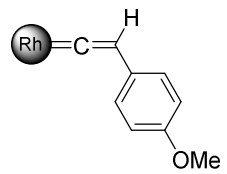	6.17

[a] Average chemical shift value for the proton atom in the vinylidene group that is attached on the surface of the Rh nanoparticles.

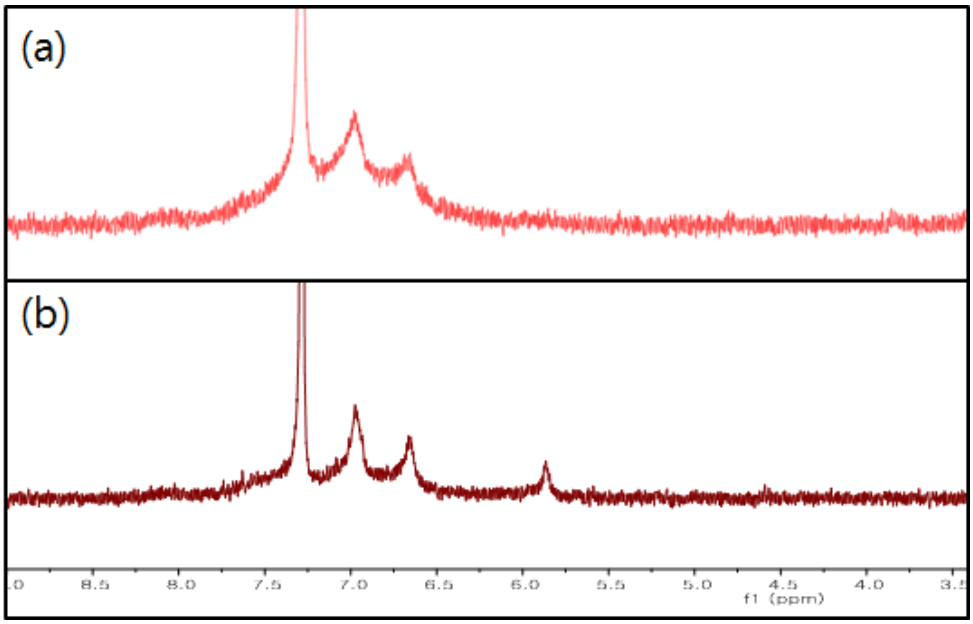

Figure S1. NMR spectra of (a) the vinylidene-functionalized Rh nanoparticles with phenylacetylene-D and (b) the vinylidene-functionalized Rh nanoparticles with phenylacetylene.

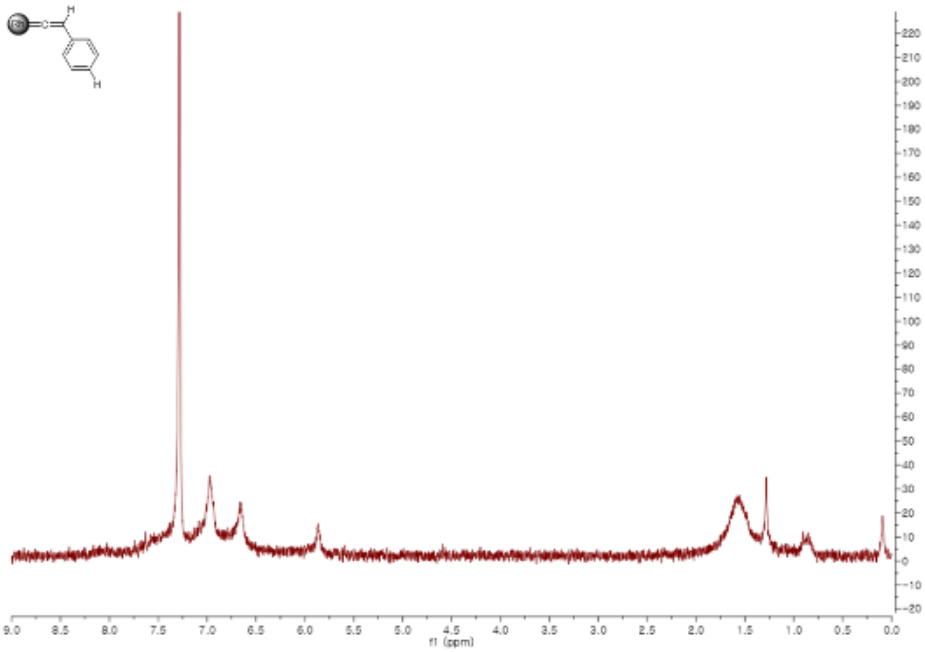

Figure S2. NMR spectra of the vinylidene-functionalized rhodium nanoparticles with phenylacetylene.

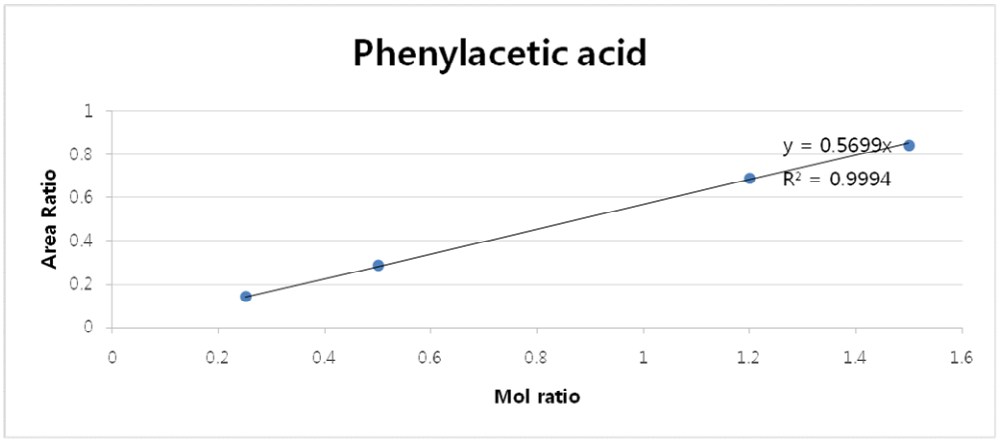

Figure S3. Calibration Curve of phenylacetic acid with *n*-dodecane.

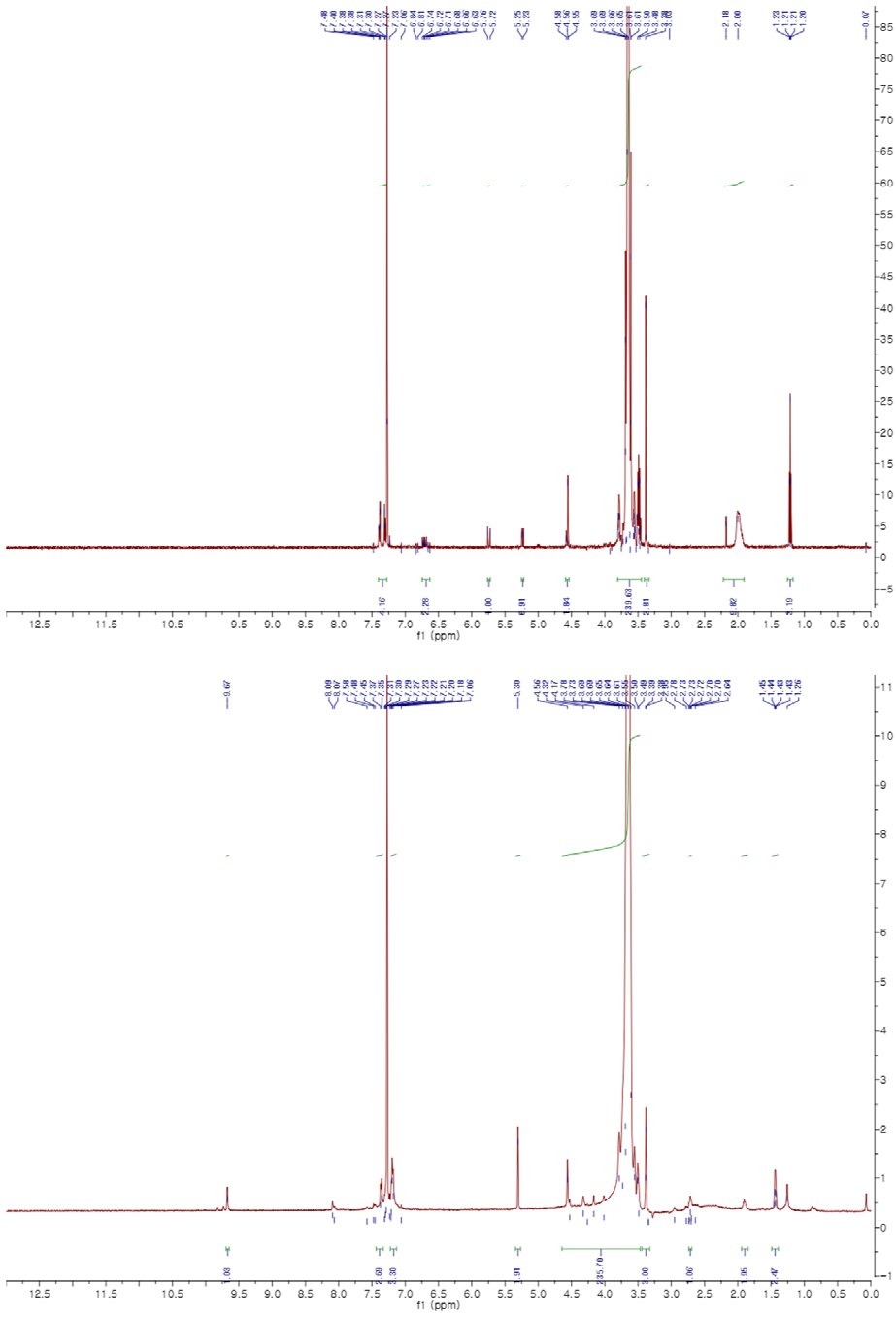

Figure S4. NMR spectra of PEG styrene before hydroformylation and after hydroformylaion reaction.

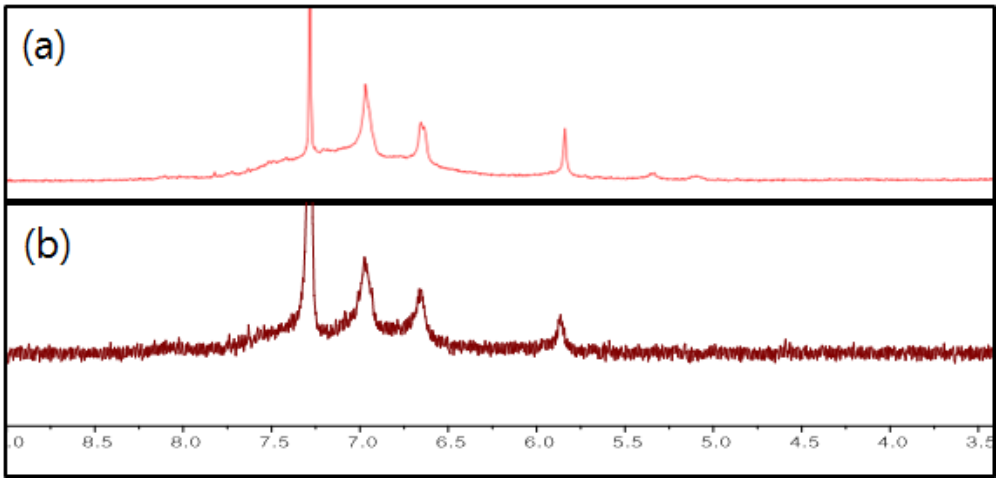

Figure S5. NMR spectra of (a) the vinylidene-functionalized Rh nanoparticles with phenylacetylene after the hydroformylation reaction and (b) the vinylidene-functionalized Rh nanoparticles with phenylacetylene before the reaction.

1H NMR data for products

2-(4-methylphenyl)propanal[17] ^{1}H NMR ($CDCl_3$, 25 °C) δ: 9.69 (s, 1H); 7.22 (d, 2H); 7.13 (d, 2H); 3.62 (q, 1H); 2.38 (s, 3H); 1.45 (d, 3H).

3-(4-methylphenyl)propanal[17] ^{1}H NMR ($CDCl_3$, 25 °C) δ: 9.81 (t, 1H); 7.12-7.07 (m, 4H); 2.92 (t, 2H); 2.76 (t, 2H); 2.32 (s, 3H).

2-(4-(trifluoromethyl)phenyl)propanal[18] ^{1}H NMR ($CDCl_3$, 25 °C) δ: 9.71 (d, 1H); 7.65 (d, 2H); 7.36 (d, 2H); 3.74 (q, 1H); 1.50 (d, 3H).

3-(4-trifluoromethyl)phenyl)propanal[19] ^{1}H NMR ($CDCl_3$, 25 °C) δ: 9.81-9.82 (t, 1H); 7.53-7.55 (d, 2H); 7.30-7.32 (d, 2H); 2.98-3.03 (m, 2H); 2.78-2.84 (m, 2H).

2-(4-(tert-butyl)phenyl)propanal[20] ^{1}H NMR ($CDCl_3$, 25 °C) δ: 9.68 (d, 1H); 7.41 (ddd, 2H); 7.15 (ddd, 2H); 3.61 (dq, 1H); 1.44 (d, 3H); 1.32 (s, 9H)

3-(4-(tert-butyl)phenyl)propanal[21] ^{1}H NMR ($CDCl_3$, 25 °C) δ: 9.83-9.84 (t, 1H); 7.32-7.35 (m, 2H); 7.14-7.16 (m, 2H); 2.92-2.98

(br m, 2H); 2.76-2.82 (m, 2H); 1.33 (s, 9H).

2-methyl-3-phenylpropanal[22] ^{1}H NMR ($CDCl_3$, 25 °C) δ: 9.72 (d, 1H); 7.17-7.34 (m, 5H); 3.07-3.14 (m, 1H); 2.57-2.75 (m, 2H); 1.10 (d, 3H)

4-phenylbutanal[23] ^{1}H NMR ($CDCl_3$, 25 °C) δ: 9.74 (t, 1H), 7.29 (t, 2H), 7.22-7.17 (m, 3H), 2.66 (t, 2H), 2.44 (td, 2H), 1.97 (q, 2H)

2-(4-chlorophenyl)propanal[17] ^{1}H NMR ($CDCl_3$, 25 °C) δ: 9.58 (d, 1H); 7.27 (d, 2H); 7.07 (d, 2H); 3.55 (dq, 1H); 1.36 (d, 3H).

3-(4-chlorophenyl)propanal[17] ^{1}H NMR ($CDCl_3$, 25 °C) δ: 9.81 (s, 1H); 7.12-7.23 (dd, 4H); 2.92 (t, 2H); 2.78 (q, 2H).

Reference

(1) (a) White, R. J.; Luque, R.; Budarin, V. L.; Clark, J. H.; Macquarrie, D. J. *Chem. Soc. Rev.* **2009**, *38*, 481-494. (b) Sperling, R. A.; Parak, W. J. *J. Phil. Trans. R. Soc. A.* **2010**, *368*, 1333-1383.

(2) (a) Quintana, M.; Vazquez, E.; Prato, M. *Acc. Chem. Res.* **2013**, *46*, 138 - 148. (b) Hirsch, A. *Angew. Chem. Int. ed.* **2002**, *41*, 1853 - 1859. (c) Tasis, D.; Tagmatarchis, N.; Bianco, A.; Prato, M. *Chem. Rev.* **2006**, *106*, 1105 - 1136.

(3) (a) Voiry, D.; Goswami, A.; Kappera, R.; Silva, C. D. C. C. E.; Kaplan, D.; Fujita, T.; Chen, M.; Asefa, T.; Chhowalla, M. *Nat. chem.* **2015**, *7*, 45 - 49. (b) Jiang, S.; Butler, S.; Bianco, E.; Restrepo, O. D.; Windl, W.; Goldberger, J. E. *Nat. Commun.* **2014**, *5*, 3389.

(4) (a) Abu-Reziq, R.; Alper, H.; Wang, D.; Post, M. L. *J. Am. Chem. Soc.* **2006**, *128*, 5279. (b) Astruc, D.; Lu, F.; Aranzaes, J. R. *Angew. Chem. Int. ed.* **2005**, *44*, 7852 - 7872.

(5) (a) Jun, S. W.; Shokouhimehr, M.; Lee, D. J.; Jang, Y.; Park, J.; Hyeon, T. *Chem. Commun.* **2013**, *49*, 7821 - 3. (b) Kesanli, B.; Lin, W. *Chem. Commun.* **2004**, 2284 - 2285. (c)

Margelefsky, E. L.; Zeidan, R. K.; Davis, M. E. *Chem. Soc. Rev.* **2008**, *37*, 1118 - 1126.

(6) Kang, X.; Zuckerman, N. B.; Konopelski, J. P.; Chen, S. *J. Am. Chem. Soc.* **2012**, *134*, 1412 - 1415.

(7) Hurst, E. C.; Wilson, K.; Fairlamb, I. J. S.; Chechik, V. *New J. Chem.* **2009**, *33*, 1837-1840.

(8) Grotjahn, D. B.; Zeng, X.; Cooksy, A. L.; Kassel, W. S.; DiPasquale, A. G.; Zakharov, L. N.; Rheingold, A. L. *Organometallics* **2007**, *26*, 3385 - 3402.

(9) Grass, M. E.; Zhang, Y.; Butcher, D. R.; Park, J. Y.; Li, Y.; Bluhm, H.; Bratlie, K. M.; Zhang, T.; Somorjai, G. a *Angew. Chem. Int. ed.* **2008**, *47*, 8893 - 8896.

(10) Hens, Z.; Martins, J. C. *Chem. Mater.* **2013**, *25*, 1211 - 1221.

(11) (a) Werner, H.; Schwab, P.; Mahr, N.; Wolf, J. *Chem. Ber.* **1992**, *125*, 2641-2650. (b) Blanchini, C.; Meli, A.; Peruzzini, M.; Zanobini, F. *Organometallics* **1990**, *9*, 241-250. (c) Cowley, M. J.; Lynam, J. M.; Whitwood, A. C. *J. Organometal. Chem.* **2010**, *695*, 18-25. (d) Cowley, M. J.; Lynam, J. M.; Slattery, J. M. *Dalton Trans.* **2008**, 4552-4554.

(12) Kim, I.; Lee, C. *Angew. Chem. Int. ed.* **2013**, *52*, 10023 -

6.

(13) (a) Cornils, B.; Herrmann, W. A. Applied Homogeneous Catalysis with Organometallic Compound, Wiley-VCH, Weinheim, 2000. (b) Leeuwen, P. W. N. M. V.; Claver, C. Rhodium Catalyzed Hydroformylation, Kluver Academic Publishers, Dordrecht, 2000. (c) Cornils, B.; Herrmann, W. A.;Rasch, M. *Angew. Chem. Int. Ed.* **1994**, *33*, 2144-2163.

(14) (A) Collman, J. P.; Hegedus, L. S.; Cooke, M. P.; Norton, J. R.; Dolcetti, G.; Marquardt, D. N. *J. Am. Chem. Soc.* **1972**, *94*, 1789-1790. (b) Witesides, G. M.; Hackett, M.; Brainard, R. L.; Lavalleye, J.-P. P. M.; Sowinski, A. F.; Izumi, A. N.; Moore, S. S.; Brown, D. W.; Staudt, E. M. *Organometallics* **1985**, *4*, 1819-1830.

(15) Hua, F.; Jiang, X.; Li, D.; Zhao, B. *Jouranl of Polymer Science: Part A: Polymer Chemistry*, **2006**, *44*, 2454-2467.

(16) Hong, S. H.; Grubbs, R. H.; *J. Am. Chem. Soc.* **2006**, *128*, 3508-3509.

(17) Christensen, S. H.; Olsen, E. P. K.; Rosenbaum, J.; Madsen, R. *Org. Biomol. Chem.* **2015**, *13*, 938-945.

(18) Friest, J. A.; Maezato, Y.; Broussy, S.; Blum, P.; Berkowitz, D. B. *J. Am. Chem. Soc.* **2010**, *132*, 5930-5931.

(19) Morimoto, T.; Fujii, T.l Miyoshi, K.; Makado, G.; Tanimoto, H.; Nishiyama, Y.; Kakiuchi, K. *Org. Biomol. Chem.* **2015**, *13*, 4632-4636.

(20) Baumann, T.; Vogt, H.; Braese, S. *Eur. J. Org. Chem.* **2007**, 266-282.

(21) Millet, A.; Baudoin, O. *Org. Lett.* **2014**, *16*, 3998-4000.

(22) Zhang, X.; Cao, B.; Yu, S.; Zhang, X. *Angew. Chem. Int. Ed.* **2010**, *49*, 4047-4050.

(23) Ghosh, A.; Nicponski, D. R. *Org. Lett.* **2011**, *13*, 4328-4331.

요 약 문

촉매 반응에서 공유 결합을 이용한 나노 물질의 활성화는 많은 연구자들에게 있어 반응 중에 나타날 수 있는 나노 촉매 간의 불필요한 상호작용을 억제시킬 수 있는 해결책 중 하나로써 각광받아왔다. 이 중에서도 균일 촉매 반응에서 금속과 잘 분리되지 않는 탄소계 리간드로 변환되는 비닐리덴 리간드를 이용하여 나노 물질을 이용한 촉매 개발을 진행하게 되었다. 이 논문에서 우리는 성공적으로 비닐리덴으로 활성화된 로듐 나노 입자를 합성하였고, 다양한 분석장비들을 이용하여 이를 분석하는데 성공했다. 특히, NMR을 이용한 연구와 촉매 표면에서 일어나는 반응을 통해서 표면에 붙어 있는 비닐리덴 리간드를 확인할 있었다. 이렇게 만들어 진 로듐 나노 입자를 히드로포밀화 반응에 적용하였다. 우리는 촉매 반응을 통해 로듐 나노 입자가 훌륭한 활성도를 지닌다는 것과, 촉매를 분리하여 재사용 실험을 진행해 본 결과 다른 계면활성제나 리간드가 붙어 있는 나노 입자들에 비해 더 안정하다는 것을 확인할 수 있었다. 또한, 로듐 나노 입자의 표면에 붙은 비닐리덴 리간드의 변화를 줌으로써 나노 입자의 활성도에 차이를 줄 수 있다는 것 역시 확인할 수 있었다.

주요어 : 비닐리덴을 이용한 활성화; 로듐 나노 입자; 표면에서의 반응; 촉매 반응의 적용; 안정성

학 번 : 2012-23044

이학 석사 학위논문

Highly Stable Rhodium Nanoparticles Functionalized by Vinylidene Group:

Synthesis, Surface Reaction, and Catalysis

Vinylidene기로 활성화된 안정한 로듐 나노입자:

합성, 표면에서의 반응, 그리고 촉매 반응

2015년 8월

서울대학교 대학원

화학부 유기화학

박 상 승

Highly Stable Rhodium Nanoparticles Functionalized by Vinylidene Group: Synthesis, Surface Reaction, and Catalysis

Vinylidene기로 활성화된 안정한 로듐 나노입자: 합성, 표면에서의 반응, 그리고 촉매 반응

지도교수 Soon Hyeok Hong
이 논문을 이학석사학위논문으로 제출함
2015년 6월
서울대학교 대학원

화학부 유기화학
박 상 승
박상승의 석사학위논문을 인준함

2015년 8월

위 원 장 이 철 범 (인)
부 위 원 장 Soon Hyeok Hong(인)
위 원 정 영 근 (인)

Abstract

Highly Stable Rhodium Nanoparticles Functionalized by Vinylidene Group: Synthesis, Surface Reaction, and Catalysis

Sangseung Park

Chemistry Department, Organic Chemistry

The Graduate Schol

Seoul National University

Covalent functionalization of nanomaterials in the catalysis have been fascinated by many researchers as one of the solutions to the problems evoked by prohibiting the unnecessary interaction between the catalysts during the reactions. Above all, we focused on the vinylidene ligand, which had been resulted in transformation to other carbon-based ligands which had not been released from the metal fragment in homogeneous catalysis, for the development with catalytic applications of the nanomaterials. In this paper, we successfully synthesized vinylidene functionalized rhodium nanoparticles and characterized them

using several tools. Especially, for the confirmation of the vinylidene group on the surface, we showed the NMR study, and surface reaction. After the characterization, we applied the vinylidene functionalized rhodium nanoparticles to the hydroformylation reaction. In the catalytic application, we showed that the rhodium nanoparticles had the excellent activity in the hydroformylation reaction and the nanoparticles is more stable than the nanoparticle using other surfactant or ligand by recycle test. And also, we showed the difference of the catalytic activity according to the vinylidene species.

Keyword : functionalization by vinylidene; rhodium nanoparticle; surface reaction; catalytic application; stability

KeywordStudent Number : 2012-23044

Table of Contents

List of Figures

List of Tables

List of Schemes

Introduction

Since 1990s, nanoparticles have been to the fore by the material scientists due to unusual properties and the synthetic method of nanoparticles has been developed using various ligand, like amine, phosphate, thiol and carboxylic acid, because the size, shape, morphology and surface properties of the nanoparticles could be changed according to the ligand[1]. Relatively recently, covalent functionalization of nanomaterials has been fascinated by many researchers because it gives an opportunity to tune the electronic and optical properties by simply modifying the surface without changing the core[2]. As a considerable numbers of studies have been conducted on the covalent functionalization of carbon-based materials[2], the interest on the covalent functionalization of inorganic nanomaterials has been tremendously increased[3]. In the catalysis field, many research group proposed the covalent fixation of catalyst on the surface of inorganic nanomaterials to utilize their high surface area[4]. By forming the rigid bond between the catalyst and inorganic support, the activity and stability of catalyst was secured by prohibiting the unnecessary interaction between the catalysts during the reaction[5]. In case of using the inorganic core as a

catalyst, however, only few reports were made regarding the covalent functionalization. Recently, The S. Chen group reported the synthesis of vinylidene functionalized Ru nanoparticles[6] and demonstrated that the metal-vinylidene bond formation could be easily achieved by introducing the alkyne derivatives during ligand exchange process. Inspired by this work, we adopted the mechanism of vinylidene functionalization to synthesize vinylidene functionalized Rh nanoparticles, which is known as an intimate counterpart of rutheniumin catalysis, and successfully utilized as a hydrformylation reaction catalyst.

From the best of our knowledge, this is the first report using vinylidene functionalized Rh nanoparticle using as a catalyst. Furthermore, the synthesized nanoparticles showed high stability through the multiple recycled reactions, which is contrast to the previously reported carbene functionalized nanoparticles[7].

Results and discussion

We successfully synthesized vinylidene functionalized Rh nanoparticles via 1,2-propandiol reduction, followed by ligand exchange process (the detailed synthetic procedures are described in the supporting information). In typical synthesis, rhodium(III) chloride hydrate, sodium acetate trihydrate and 1,2-propanediol were stirred gently for 30 min at room temperature. The temperature of mixture solution was increased until it reaches to 165 °C, and kept at this temperature for 2hr. At this point, the color of mixture solution turned complete black from transparent yellow, which indicates the rhodium nanoparticles were formed with the help of 1,2-propandiol and the sufficiently high temperature. After the reaction termination, the mixture solution was cooled down to room temperature and rinsed excessively with the mixture of methanol and ethanol. To attach vinylidene ligand on the surface of Rh nanoparticles, acetylene terminated ligands were introduced to the nanoparticles dispersed in toluene at the ratio of 1mmol ligand per 1mg of nanoparticles (typically, we used phenylacetylene for the model reactions). This procedure leads to the formation of intermediate η^2-alkyne complex on the Rh nanoparticle surface, which result in rearrangement to the η

[1]-vinylidene via 1,3-H shifts[8]. The reaction mixture was kept at room temperature for overnight with vigorous stirring. The resulting products were rinsed again with methanol and ethanol to remove residual unreacted organic ligands. After the washing process, vinylidene functionalized Rh nanoparticles were dried at the vacuum oven for an hour.

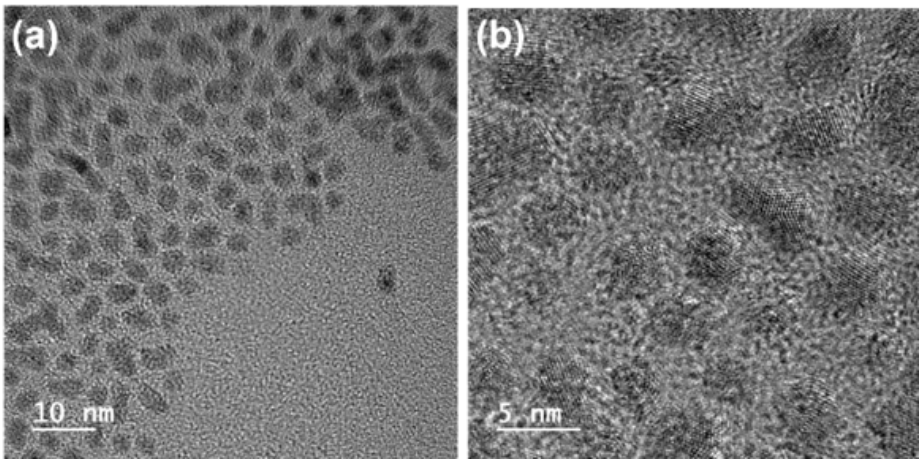

Figure 1. TEM images of vinylidene functionalized Rh nanoparticles.

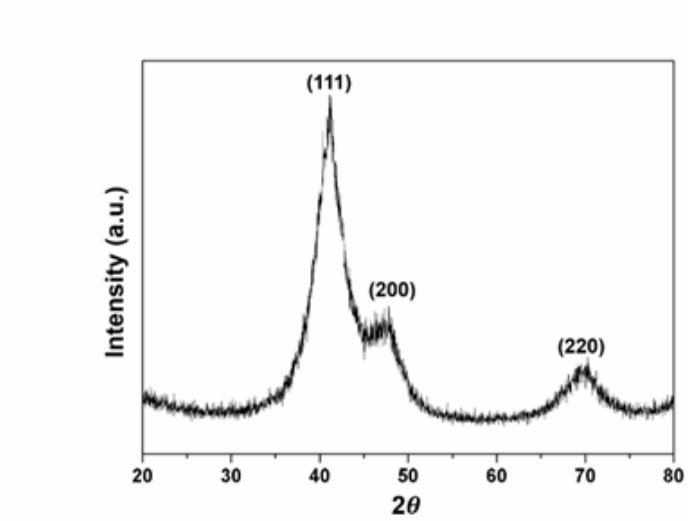

Figure 2. The powder X-ray diffraction (XRD) pattern of the synthesized catalyst (PDF#: 05-0685).

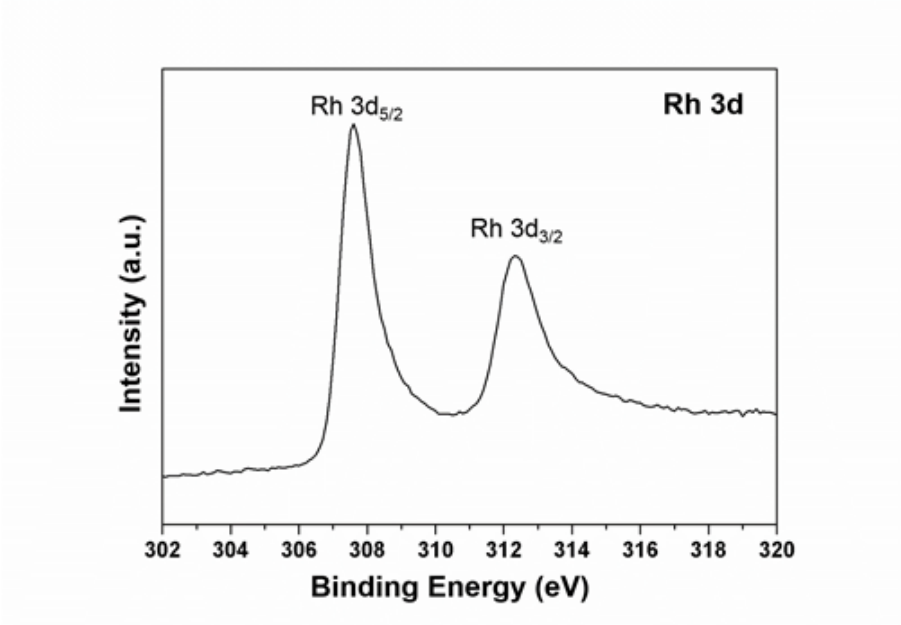

Figure 3. Rh 3d X-Ray photoelectron spectra of the vinylidene functionalized Rh nanoparticles.

Transmission electron microscope (TEM) images of the synthesized nanoparticles reveal that the size range of nanoparticles were 3 to 4 nm (Figure 1), and the powder X-ray diffraction (XRD) pattern shows that the oxidation state of the nanoparticles is Rh^0 (Figure 2). Since catalytic reaction only occurs on the surface of heterogeneous catalyst, we confirmed that the surface of synthesized Rh nanoparticles were also close to Rh^0 from X-ray photoelectron spectra (Figure 3). The Rh 3d spectra indicates (the binding energy of Rh 3d5/2 at 307.5 and Rh 3d3/2 at 312.3) that the surface of as-synthesized Rh

nanoparticles were Rh^0 (the binding energy of Rh 3d5/2 at 307.3 and Rh 3d3/2 at 312.0) while binding energies of Rh2O3 has 308.4 at Rh 3d5/2 and 313.3 at Rh 3d3/2. The partial oxidation of Rh nanoparticles, leading peaks shift to the higher binding energies, was inevitable due to the size effect, which is previously reported phenomena[9].

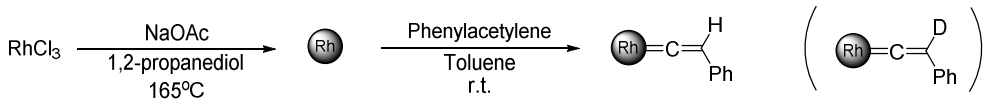

Scheme 1. Synthesis of vinylidene functionalized rhodium nanoparticles with phenylacetylene-D.

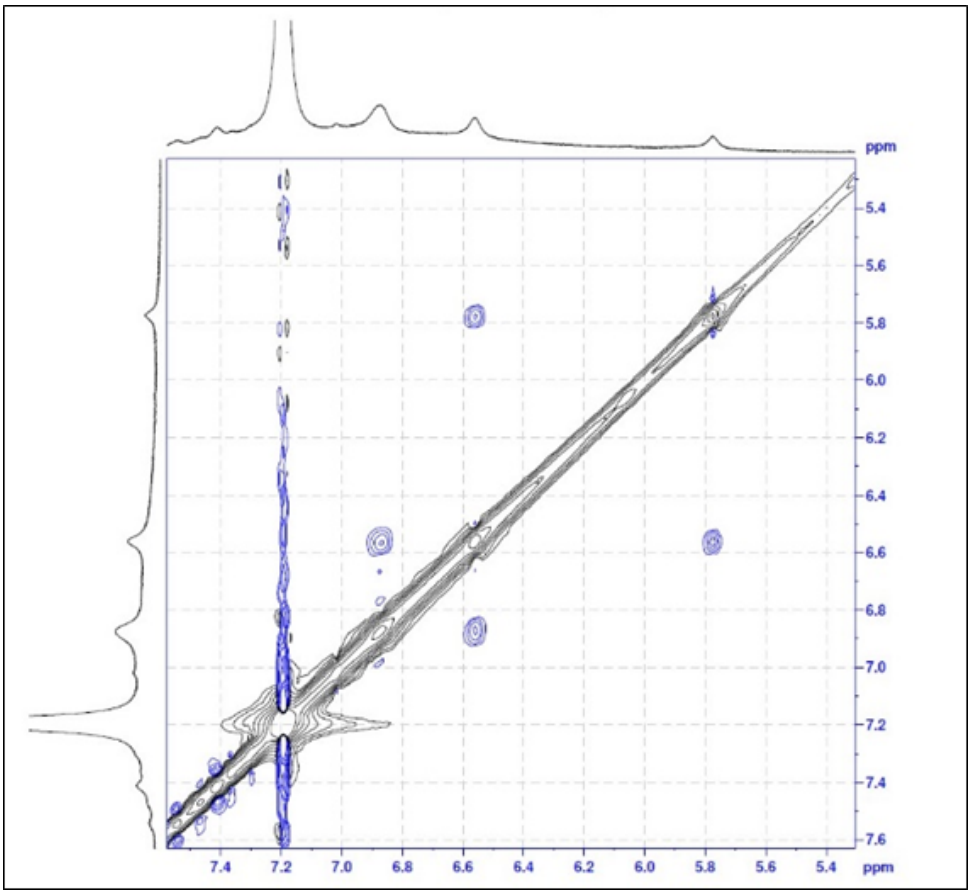

Figure 4. The rotating frame overhause effect spectroscopy of the Rh nanoparticles.

Due to the peak broadening of 1H proton NMR, the peaks could not be exactly assigned. This is a generally observed phenomenon in the NMR spectra of ligands tightly bound on the surface of nanoparticles[10] (Figure S2a). Thus, we performed rotating frame overhause effect spectroscopy (ROESY) NMR analysis to verify the existence of the vinylidene group on the

surface of Rh nanoparticles. Generally, the NMR peak of the proton, which is located on the vinylidene group, is existed at 4 to 0 ppm in 1H-NMR spectroscopy and the peak was shifted to down-field as rhodium metal is more electron-rich[11]. The ROESY NMR data showed that the proton of vinylidene group, the peak at 5.85 ppm, was strongly interacting with the protons of phenyl rings. To confirm that the peak at 5.85 ppm correspond to the proton of vinylidene group, we performed the ligand exchange process with the deuterium substituted phenylacetylene (phenylacetylene-D, Scheme 1). As expected, the intensity of peak at 5.85 ppm was decreased while the other phenyl ring peaks showed unchanged. As a result, we concluded that the peak at 5.85 ppm correspond to the proton of vinylidene group. This vinylidene proton peak could be shifted to upfield or downfield depending on the electron-richness of phenyl ring. When fluorine group or methyl group was located on the para position, the vinylidene proton was shifted to upfield (5.75 ppm or 5.81 ppm) (Table S1). However, the peak of vinylidene proton was shifted to downfield (6.17 ppm) in the case of 4-methoxy phenylacetylene, which indicates that position of vinylidene proton peak was strongly affected by the electron-richness of phenyl ring.

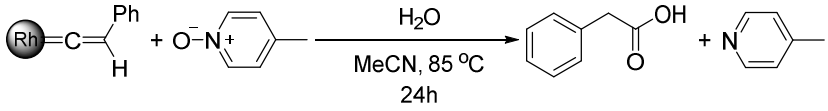

Scheme 2. C-O oxidation reaction.

Further, we performed an oxgenative addition reaction on surface to check if vinylidene groups are properly functionalized on the Rh nanoparticle surface (Scheme 2). In a recent study, the C. Lee group demonstrated rhodium-catalyzed oxygenative addition reaction to terminal alkynes, which involves formation of a rhodium vinylidene complex, for the synthesis of carboxylic acids[12]. Mechanistically, η^1-isomer of the π-alkyne rhodium complex is essential to yield ketene from the oxygenation of vinylidene complex (Figure 5). We used 4-picoline N-oxide as an oxygen donor and water as a nucleophile to confirm the identity of vinylidene functionalization conclusively, with a fundamental question of whether such reaction can take place on the surface of nanoparticles. To our delight, we observed phenylacetic acid from the oxygenative addition reaction on surface, signifying vinylidene groups were successfully functionalized on the surface of Rh nanoparticles. To quantify the yield (90 %) of the reaction, we got the CHNS data of Rh nanoparticles and compared to the result of the oxygenative addition reaction. Using this method, we could quantify the amount of vinylidene functionalization on Rh nanoparticles. Thus,

we concluded that the Rh nanoparticles were successfully functionalized with the vinylidene group.

Since the hydroformylation reaction was discovered by Otto Roelen in 1938, this reaction is the largest homogeneous catalytic process in industry, which produce more 15 billion pounds of aldehydes or alcohols per year, and, although the process was well developed since 1938, many researchers have been interested in hydroformylation reaction for the improvement of the selectivity to linear or branched products and the activity in mild conditions[13]. Vinylidene functionalized Rh nanoparticle showed excellent activity towards hydroformylation reaction starting with various substrates (Table 1). For the styrene derivatives, para-substituted compounds were successfully converted to the corresponding products regardless of electron-donating or -withdrawing groups with branched form aldehyde as a major product. Interestingly, CF_3 substituted styrene showed the highest regioselectivity while the other electron withdrawing group, chlorine, substituted styrene showed the similar regioselectivity with the model reaction. Unfortunately, our rhodium nanoparticle was not active for the hydroformylation of internal olefin, but terminal aliphatic compound showed complete conversion of reaction product with the linear-formed aldehyde as a major product.

TABLE 1. Substrate scope of hydroformylation reaction[a]

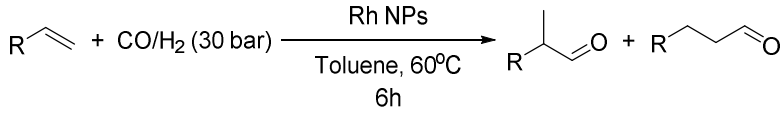

Entry	Substrate	Conversion (%)[b]	Selectivity (*b:l*)[b]
1	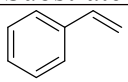	100[c]	84.3 : 15.7
2	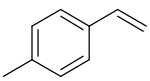	82	74.9 : 25.1
3	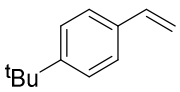	100	79.1 : 20.9
4	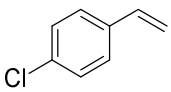	100	75.2 : 24.8
5	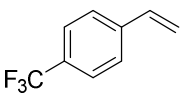	83	97.0 : 3.0
6	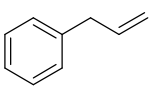	100	30.0 : 70.0
7	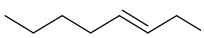	0	-

[a] Hydroformylation condition: olefin (10 mmol), Rh nanoparticles (10.2 mg), toluene (10 ml), CO (initial pressure, 15 bar), H_2 (initial pressure, 15 bar), reaction temperature (60°C), and reaction time (6 h). [b] Conversion and selectivity were determined by ^{1}H NMR. [c] Conversion and selectivity in entry 1 were determined by gas chromatography using dodecane as an internal standard.

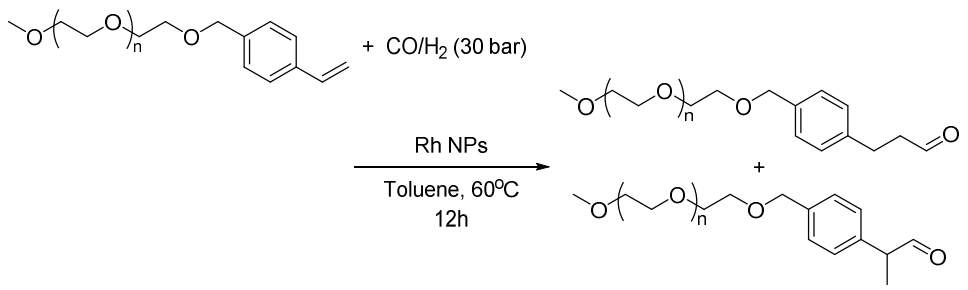

Scheme 3. Three phase reaction.

To show this is a complete heterogeneous reaction, we performed designed reaction called 'three phase reaction' (Scheme 3)[14]. Basic idea of the study is to know if this reaction is going with leached out metal moiety or fully running with the heterogeneous nanoparticles by comparing the reaction completion time, using two different types of substrates. One reaction starts with a substrate attached to the insoluble support while the other reaction starts with an analogous soluble substrate. If the reaction only proceeds with the heterogeneous catalyst, the supported substrate will react much slower than the freestanding soluble substrate. Conversely, there will be no difference in the completion time between the designed reactions, in case of leached out catalyst plays a major role to complete the reaction. We immobilized styrene to (Polyethyleneglycol)-methyl ether and used as an insoluble supported substrate. As expected, it took more than 2 days to complete the reaction while it required only

6 hr to complete the reaction with an analogous soluble substrate. Thus, we concluded that the reaction was running under the heterogeneous nanoparticle surface, and there is no leaching effect.

It is well known that the commonly reported nanocatalysts immediately aggregate after the chemical reactions due to the weak binding of ligand on the nanoparticle surface. However, phenylacetylene functionalized Rh nanoparticle showed excellent dispersion after the hydroformylation reaction, while phenylacetic acid and acetate functionalized Rh nanoparticles precipitated even after the long time sonication as shown in Figure 5a. Thanks to the rigid covalent bond formation of organic ligand on the nanoparticle surface, dispersibility of the nanoparticle maintained through the multiple recycling process with high conversion and selectivity (Table 2). After the reaction, no significant particle aggregation or morphology transformation was observed (Figure 5b) and there was similar pattern of Rh 3d X-Ray photoelectron spectra of the vinylidene functionalized Rh nanoparticles (Figure 5C). And also, using 1H-NMR spectroscopy, we confirmed that the vinylidene proton was remained at the hydroformylation reaction condition. We also tested oleic acid, frequently used surfactant in the nanoparticle synthesis, passivated Rh nanoparticles, and it also gave us high conversion and selectivity

at the initial trial. However, activity of the catalyst rapidly dropped after the 2nd or 3rd trial, and it became permanently inactive before 5th recycle.

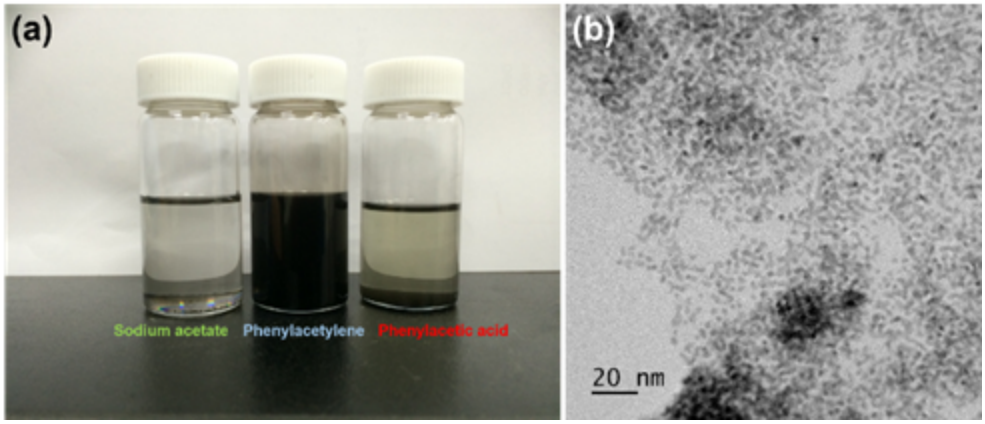

Figure 5. (a) Picture of the catalyst dispersed in the substrate mixture solution before the 2nd recycle. (b) TEM image of the phenylacetylene functionalized Rh nanoparticles after the 1st reaction termination.

Table 2. Recycling results of the phenylacetylene, phenylacetic acid and oleic acid passivated Rh nanocatalysts[a]

Recycle #	Ligand					
	Phenylacetylene		Phenylacetic acid		Oleic acid	
	Conv. (%)	Sel. (b/l)	Conv. (%)	Sel. (b/l)	Conv. (%)	Sel. (b/l)
1	100	5.4	61	4.6	92	6.9
2	100	5.2	45	9.1	87	8.4
3	100	5.6	23	20.3	47	13.7
6	99	5.5				
8	96	6.2				

[a] Conditions: styrene (1.15 ml, 10 mmol), Rh nanoparticles (10.2 mg), toluene (10 ml), CO (initial pressure, 15 bar), H_2 (initial pressure, 15 bar), reaction temperature (60°C), reaction time (6 h), and conversion and selectivity were determined by gas chromatography using dodecane as an internal standard.

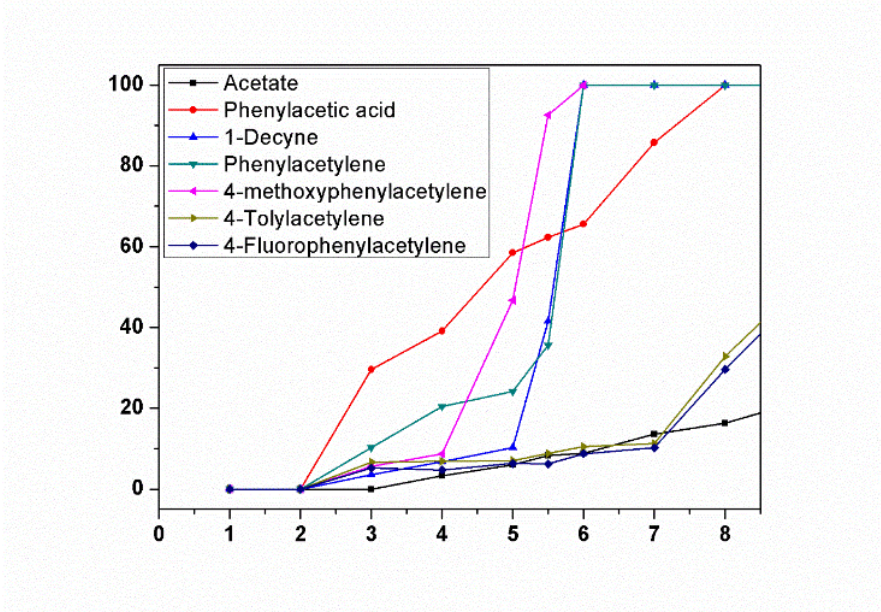

Figure 6. Time-dependent product yield of the hydroformylation reaction using Rh nanoparticles passivated with various ligands.

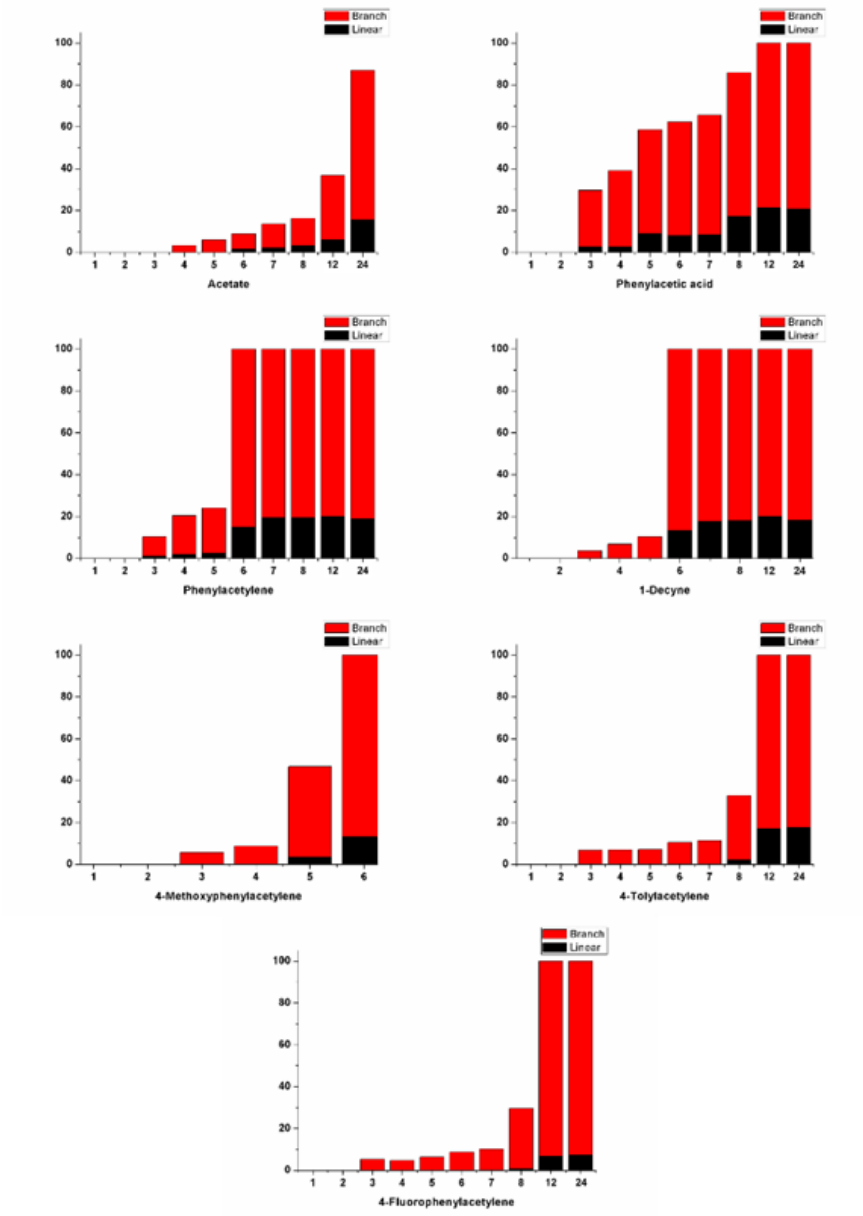

Figure 7. Time-dependent product yield and selectivity of the hydroformylation reaction using Rh nanoparticles passivated with various ligands. (X-axis: conversion, Y-axis: time (h))

By varying the passivating ligand on the surface of Rh nanoparticles via ligand exchange process, it was able to control the reaction kinetics of hydroformylation reaction. To obtain the reaction kinetics profile, we ran the hydroformylation reactions with various vinylidene or carboxylate ligands passivated Rh nanoparticles under identical conditions. During the reaction, aliquots were drawn from the reaction mixtures at an hour interval, and the results are shown on Figure 6 and Figure 7. From the reaction profile, at least three aspects were observed. First, vinylidene functionalized Rh nanoparticle involved hydroformylation reaction required induction time before the rapid conversion of reaction product while carboxylate functionalized ones showed the steady increase of reaction product. Secondly, only branched form was produced at the early stage of the reaction, before it reaches 20% conversion. Ratio of the linear product increase as the reaction proceeds, but never exceeded a certain level. Lastly, each of vinylidene ligand passivated Rh nanoparticles showed different activities. Even though para-substituted phenylacetylene with methyl or fluoro group elongated reaction time, 4-methoxyphenylacetylene passivated Rh nanoparticle accelerated reaction time. The correlativity of the results are under investigation.

Conclusion

In conclusion, we successfully synthesized vinylidene functionalized rhodium nanoparticle and analyze the nanoparticle through the several tools. In the analysis process, it is the first trial of using chemical reaction for characterizing the structure between vinylidene ligand and surface of the nanoparticle. This vinylidene functionalized Rh nanoparicle showed the excellent catalytic activity for the hydroformylation reaction of styrene. As far as we know, this is also the first example of the catalytic reaction using vinylidene functionalized nanoparticles and that showed the difference of the catalytic activity according to the vinylidene species. In the stabilization issue, we found that the vinylidene functionalized rhodium nanoparticle is more stable than the nanoparticle using other surfactant or ligand and could be recycled for catalytic reaction. Based on these results, we suggest that this type of nanoparticle could be prepared using other vinylidene ligand and improve the catalytic activity for the other catalytic system.

Experimental section

Synthesis of vinylidene functionalized Rh nanopar-itcles

In typical synthesis, 100 mg of rhodium(III) chloride hydrate, 220 mg of sodium acetate trihydrate and 140 mL of 1,2-propanediol were stirred gently for 30 min at room temperature. The temperature of mixture solution was increased at the rate of 5 °C per minute until it reaches to 165 °C, and kept at this temperature for 2 hr. After the reaction termination, the mixture solution was cooled down to room temperature and rinsed excessively with mixture of methanol and ethanol. To attach vinylidene ligand on the surface of Rh nanoparticles, acetylene terminated ligands were introduced to the nanoparticles dispersed in 10 mL of toluene at the ratio of 1 mmol ligand per 1 mg of nanoparticles. The reaction mixture was kept at room temperature for overnight with vigorous stirring. The resulting products were rinsed again with methanol and ethanol to remove residual unreacted organic ligands. After the washing process, vinylidene functionalized Rh nanoparticles were dried at the vacuum oven for an hour.

Characterization of rhodium nanoparticles function-

alized with phenylacetylene through rhodium-catalyzed oxygenative addition

20 mg of rhodium nanoaparticles, 131 mg of 4-picoline *N*-oxide, 0.18 mL of water and 0.5 mL of CH_3CN were placed in vial and gently stirred for a minute. The mixture was heated to 60°C and maintained at this temperature for 24 hr. After the reaction, the mixture was filtered for the separation of nanoparticles and the products were analyzed by GC-MS using HP-5 MS column. Dodecane was used as an internal standard. For the ligand amount quantification, vinylidene functionalized Rh nanoparticles were ionized in aqua regia, then toluene was introduced to gather the organic moieties from Rh nanoparticle ionization. Upper organic mixture part was transferred to separate vial and excessively washed with water to remove any acetate ligand or residual acid protons.

General procedure of hydroformylation with Rhodium nanoparticles

10.2 mg of rhodium nanoparticles were dispersed in 10 mL of toluene, and the mixture solution was placed on the high pressure reactor with 1.15 mL of styrene. The solution was purged with CO gas for 10 min. Then, the pressure of the reactor was increased up to 30 atm that consist of 15 atm of

CO gas and 15 atm of H_2 gas. The temperature of reactor was increased until it reaches 60 °C, and maintained at this temperature for 6 hr. After the reaction, the nanoparticles were filtered by celite. The product was analyzed by GC-MS using identical column used in the oxygenative addition reaction analysis. Dodecane was used as a internal standard.

Synthesis of MeOPEG-styrene

2.93 g of (Polyethyleneglycol)-methyl ether (MW : 5000), 0.33g of sodium hydride and 5 mL of dry THF were added to a three-necked flask. The mixture was stirred under an Ar atmosphere for 1 hr. A solution consists of 0.60 g of 4-vinylbenzyl chloride and 5 mL of dry THF was added dropwise to the mixture solution and refluxed at 65 °C overnight[15]. To quench the reaction, reaction batch was cooled down to ambient temperature followed by addition of a few drops of water. THF was removed in vacuo, and 100 mL of dichloromethane was added to dissolve the product. CH_2Cl_2 solution was passed through a pad of celite. After the evaporation of volatiles, the crude mixture was eluted through a pad of silica gel using dichloromethane and methanol, and the product was precipitated from dichloromethane into diethyl ether. The precipitates were collected by a centrifuge to yield a fluffy

white solid[16].

General procedure of Three-Phase Test

500 mg of MeOPEG-styrene and rhodium nanoparticles (1 mol%) were mixed in 10 mL of toluene. Using high pressure reactor, the solution was purged with CO gas for 10 min. Then, the reactor pressure was elevated to 30 atm by injecting 15 atm of CO gas and 15 atm of H_2 gas. The reactor was heated at 60 ℃ and maintained at the given reaction time. After the reaction termination, the nanoparticles were filtered by celite. The solvent was dried in vacuo, and the product was analyzed by ^{1}H-NMR.

Supporting Information

Table S1. Comparison of Chemical Shift of the Vinylidene-proton according to para-substituted phenylacetylene.

	δ H (ppm)[a]
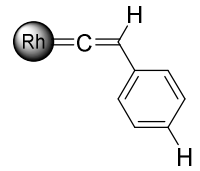	5.87
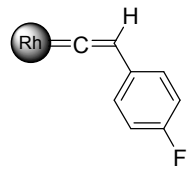	5.75
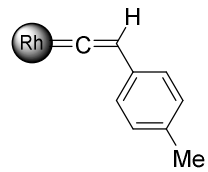	5.81
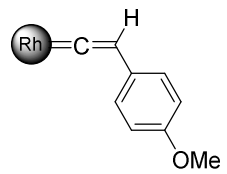	6.17

[a] Average chemical shift value for the proton atom in the vinylidene group that is attached on the surface of the Rh nanoparticles.

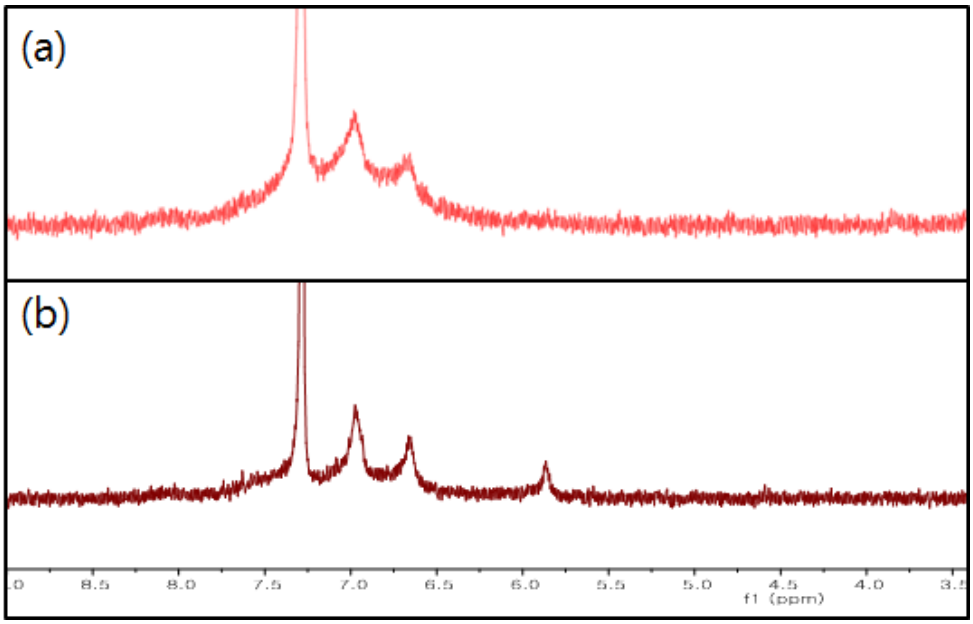

Figure S1. NMR spectra of (a) the vinylidene-functionalized Rh nanoparticles with phenylacetylene-D and (b) the vinylidene-functionalized Rh nanoparticles with phenylacetylene.

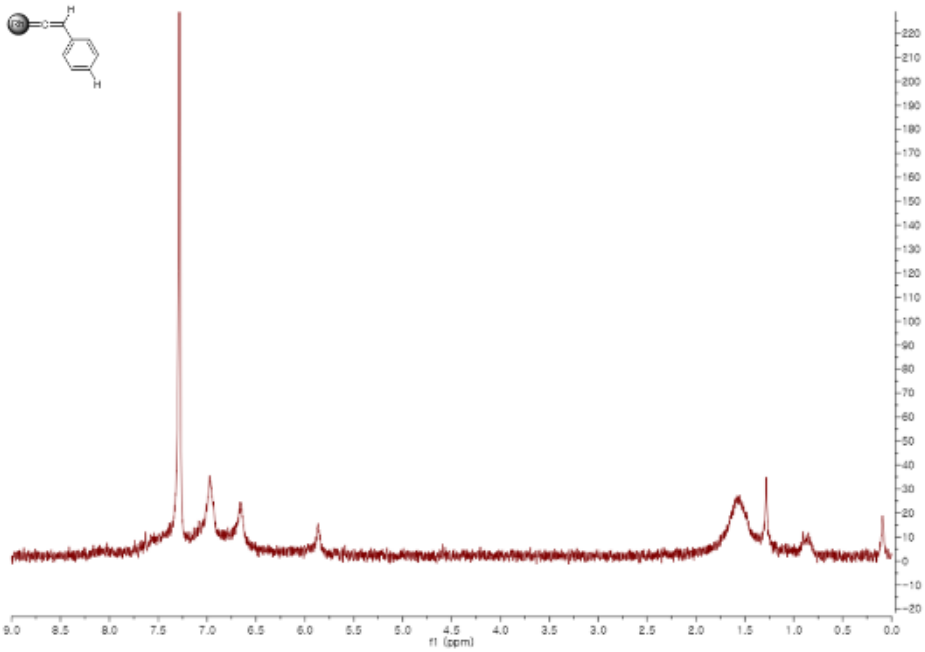

Figure S2. NMR spectra of the vinylidene-functionalized rhodium nanoparticles with phenylacetylene.

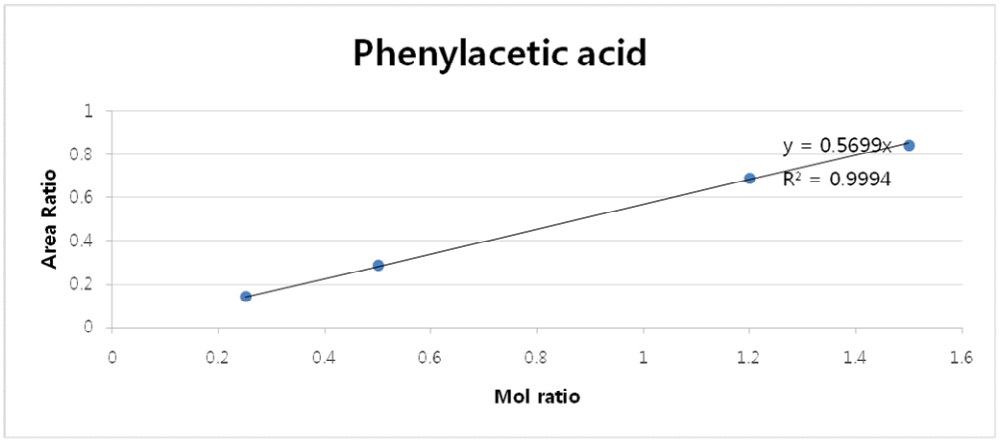

Figure S3. Calibration Curve of phenylacetic acid with *n*-dodecane.

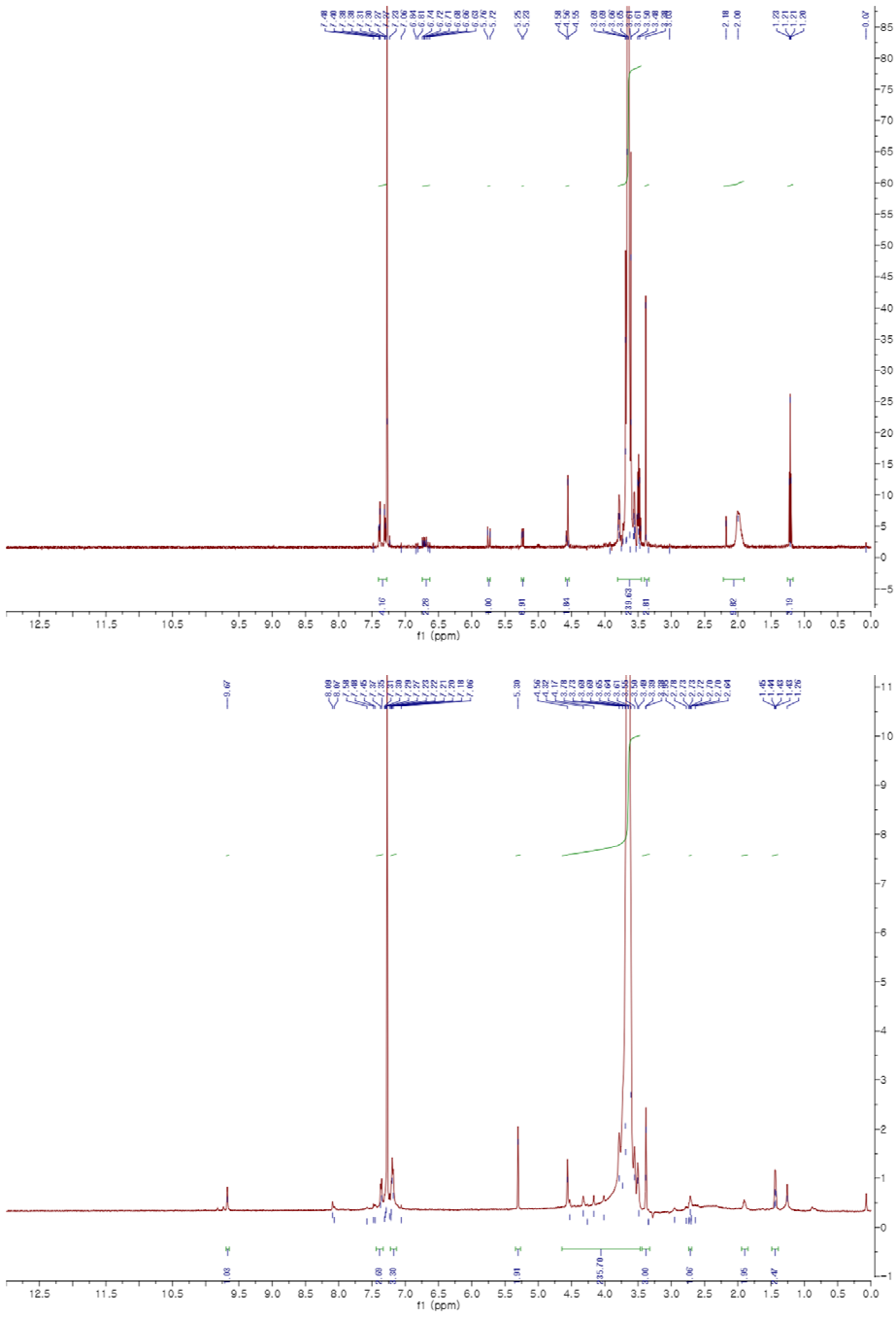

Figure S4. NMR spectra of PEG styrene before hydroformylation and after hydroformylaion reaction.

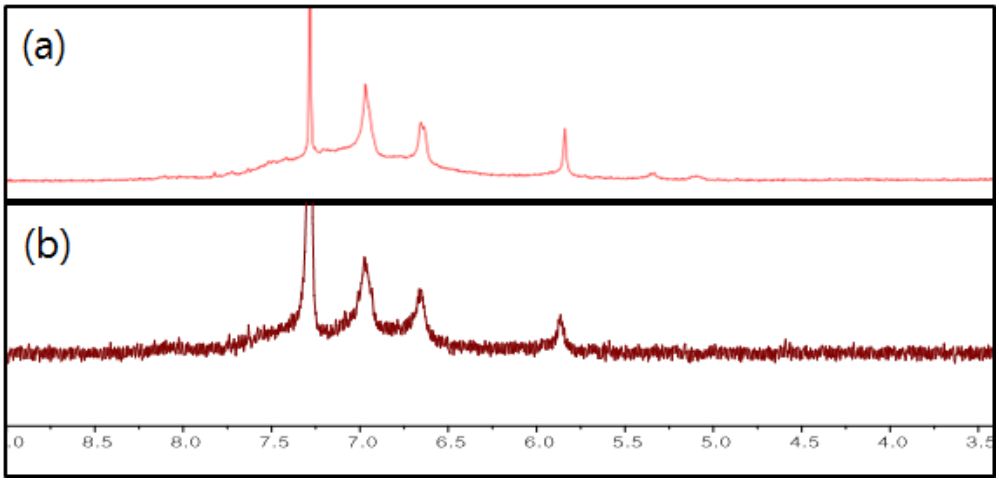

Figure S5. NMR spectra of (a) the vinylidene-functionalized Rh nanoparticles with phenylacetylene after the hydroformylation reaction and (b) the vinylidene-functionalized Rh nanoparticles with phenylacetylene before the reaction.

1H NMR data for products

2-(4-methylphenyl)propanal[17] ^{1}H NMR ($CDCl_3$, 25 °C) δ: 9.69 (s, 1H); 7.22 (d, 2H); 7.13 (d, 2H); 3.62 (q, 1H); 2.38 (s, 3H); 1.45 (d, 3H).

3-(4-methylphenyl)propanal[17] ^{1}H NMR ($CDCl_3$, 25 °C) δ: 9.81 (t, 1H); 7.12-7.07 (m, 4H); 2.92 (t, 2H); 2.76 (t, 2H); 2.32 (s, 3H).

2-(4-(trifluoromethyl)phenyl)propanal[18] ^{1}H NMR ($CDCl_3$, 25 °C) δ: 9.71 (d, 1H); 7.65 (d, 2H); 7.36 (d, 2H); 3.74 (q, 1H); 1.50 (d, 3H).

3-(4-trifluoromethyl)phenyl)propanal[19] ^{1}H NMR ($CDCl_3$, 25 °C) δ: 9.81-9.82 (t, 1H); 7.53-7.55 (d, 2H); 7.30-7.32 (d, 2H); 2.98-3.03 (m, 2H); 2.78-2.84 (m, 2H).

2-(4-(tert-butyl)phenyl)propanal[20] ^{1}H NMR ($CDCl_3$, 25 °C) δ: 9.68 (d, 1H); 7.41 (ddd, 2H); 7.15 (ddd, 2H); 3.61 (dq, 1H); 1.44 (d, 3H); 1.32 (s, 9H)

3-(4-(tert-butyl)phenyl)propanal[21] ^{1}H NMR ($CDCl_3$, 25 °C) δ: 9.83-9.84 (t, 1H); 7.32-7.35 (m, 2H); 7.14-7.16 (m, 2H); 2.92-2.98

(br m, 2H); 2.76-2.82 (m, 2H); 1.33 (s, 9H).

2-methyl-3-phenylpropanal[22] ^{1}H NMR ($CDCl_3$, 25 °C) δ: 9.72 (d, 1H); 7.17-7.34 (m, 5H); 3.07-3.14 (m, 1H); 2.57-2.75 (m, 2H); 1.10 (d, 3H)

4-phenylbutanal[23] ^{1}H NMR ($CDCl_3$, 25 °C) δ: 9.74 (t, 1H), 7.29 (t, 2H), 7.22-7.17 (m, 3H), 2.66 (t, 2H), 2.44 (td, 2H), 1.97 (q, 2H)

2-(4-chlorophenyl)propanal[17] ^{1}H NMR ($CDCl_3$, 25 °C) δ: 9.58 (d, 1H); 7.27 (d, 2H); 7.07 (d, 2H); 3.55 (dq, 1H); 1.36 (d, 3H).

3-(4-chlorophenyl)propanal[17] ^{1}H NMR ($CDCl_3$, 25 °C) δ: 9.81 (s, 1H); 7.12-7.23 (dd, 4H); 2.92 (t, 2H); 2.78 (q, 2H).

Reference

(1) (a) White, R. J.; Luque, R.; Budarin, V. L.; Clark, J. H.; Macquarrie, D. J. *Chem. Soc. Rev.* **2009**, *38*, 481-494. (b) Sperling, R. A.; Parak, W. J. *J. Phil. Trans. R. Soc. A.* **2010**, *368*, 1333-1383.

(2) (a) Quintana, M.; Vazquez, E.; Prato, M. *Acc. Chem. Res.* **2013**, *46*, 138 - 148. (b) Hirsch, A. *Angew. Chem. Int. ed.* **2002**, *41*, 1853 - 1859. (c) Tasis, D.; Tagmatarchis, N.; Bianco, A.; Prato, M. *Chem. Rev.* **2006**, *106*, 1105 - 1136.

(3) (a) Voiry, D.; Goswami, A.; Kappera, R.; Silva, C. D. C. C. E.; Kaplan, D.; Fujita, T.; Chen, M.; Asefa, T.; Chhowalla, M. *Nat. chem.* **2015**, *7*, 45 - 49. (b) Jiang, S.; Butler, S.; Bianco, E.; Restrepo, O. D.; Windl, W.; Goldberger, J. E. *Nat. Commun.* **2014**, *5*, 3389.

(4) (a) Abu-Reziq, R.; Alper, H.; Wang, D.; Post, M. L. *J. Am. Chem. Soc.* **2006**, *128*, 5279. (b) Astruc, D.; Lu, F.; Aranzaes, J. R. *Angew. Chem. Int. ed.* **2005**, *44*, 7852 - 7872.

(5) (a) Jun, S. W.; Shokouhimehr, M.; Lee, D. J.; Jang, Y.; Park, J.; Hyeon, T. *Chem. Commun.* **2013**, *49*, 7821 - 3. (b) Kesanli, B.; Lin, W. *Chem. Commun.* **2004**, 2284 - 2285. (c)

Margelefsky, E. L.; Zeidan, R. K.; Davis, M. E. *Chem. Soc. Rev.* **2008**, *37*, 1118 - 1126.

(6) Kang, X.; Zuckerman, N. B.; Konopelski, J. P.; Chen, S. *J. Am. Chem. Soc.* **2012**, *134*, 1412 - 1415.

(7) Hurst, E. C.; Wilson, K.; Fairlamb, I. J. S.; Chechik, V. *New J. Chem.* **2009**, *33*, 1837-1840.

(8) Grotjahn, D. B.; Zeng, X.; Cooksy, A. L.; Kassel, W. S.; DiPasquale, A. G.; Zakharov, L. N.; Rheingold, A. L. *Organometallics* **2007**, *26*, 3385 - 3402.

(9) Grass, M. E.; Zhang, Y.; Butcher, D. R.; Park, J. Y.; Li, Y.; Bluhm, H.; Bratlie, K. M.; Zhang, T.; Somorjai, G. a *Angew. Chem. Int. ed.* **2008**, *47*, 8893 - 8896.

(10) Hens, Z.; Martins, J. C. *Chem. Mater.* **2013**, *25*, 1211 - 1221.

(11) (a) Werner, H.; Schwab, P.; Mahr, N.; Wolf, J. *Chem. Ber.* **1992**, *125*, 2641-2650. (b) Blanchini, C.; Meli, A.; Peruzzini, M.; Zanobini, F. *Organometallics* **1990**, *9*, 241-250. (c) Cowley, M. J.; Lynam, J. M.; Whitwood, A. C. *J. Organometal. Chem.* **2010**, *695*, 18-25. (d) Cowley, M. J.; Lynam, J. M.; Slattery, J. M. *Dalton Trans.* **2008**, 4552-4554.

(12) Kim, I.; Lee, C. *Angew. Chem. Int. ed.* **2013**, *52*, 10023 -

6.

(13) (a) Cornils, B.; Herrmann, W. A. Applied Homogeneous Catalysis with Organometallic Compound, Wiley-VCH, Weinheim, 2000. (b) Leeuwen, P. W. N. M. V.; Claver, C. Rhodium Catalyzed Hydroformylation, Kluver Academic Publishers, Dordrecht, 2000. (c) Cornils, B.; Herrmann, W. A.;Rasch, M. *Angew. Chem. Int. Ed.* **1994**, *33*, 2144-2163.

(14) (A) Collman, J. P.; Hegedus, L. S.; Cooke, M. P.; Norton, J. R.; Dolcetti, G.; Marquardt, D. N. *J. Am. Chem. Soc.* **1972**, *94*, 1789-1790. (b) Witesides, G. M.; Hackett, M.; Brainard, R. L.; Lavalleye, J.-P. P. M.; Sowinski, A. F.; Izumi, A. N.; Moore, S. S.; Brown, D. W.; Staudt, E. M. *Organometallics* **1985**, *4*, 1819-1830.

(15) Hua, F.; Jiang, X.; Li, D.; Zhao, B. *Jouranl of Polymer Science: Part A: Polymer Chemistry*, **2006**, *44*, 2454-2467.

(16) Hong, S. H.; Grubbs, R. H.; *J. Am. Chem. Soc.* **2006**, *128*, 3508-3509.

(17) Christensen, S. H.; Olsen, E. P. K.; Rosenbaum, J.; Madsen, R. *Org. Biomol. Chem.* **2015**, *13*, 938-945.

(18) Friest, J. A.; Maezato, Y.; Broussy, S.; Blum, P.; Berkowitz, D. B. *J. Am. Chem. Soc.* **2010**, *132*, 5930-5931.

(19) Morimoto, T.; Fujii, T.l Miyoshi, K.; Makado, G.; Tanimoto, H.; Nishiyama, Y.; Kakiuchi, K. *Org. Biomol. Chem.* **2015**, *13*, 4632-4636.

(20) Baumann, T.; Vogt, H.; Braese, S. *Eur. J. Org. Chem.* **2007**, 266-282.

(21) Millet, A.; Baudoin, O. *Org. Lett.* **2014**, *16*, 3998-4000.

(22) Zhang, X.; Cao, B.; Yu, S.; Zhang, X. *Angew. Chem. Int. Ed.* **2010**, *49*, 4047-4050.

(23) Ghosh, A.; Nicponski, D. R. *Org. Lett.* **2011**, *13*, 4328-4331.

요 약 문

촉매 반응에서 공유 결합을 이용한 나노 물질의 활성화는 많은 연구자들에게 있어 반응 중에 나타날 수 있는 나노 촉매 간의 불필요한 상호작용을 억제시킬 수 있는 해결책 중 하나로써 각광받아왔다. 이 중에서도 균일 촉매 반응에서 금속과 잘 분리되지 않는 탄소계 리간드로 변환되는 비닐리덴 리간드를 이용하여 나노 물질을 이용한 촉매 개발을 진행하게 되었다. 이 논문에서 우리는 성공적으로 비닐리덴으로 활성화된 로듐 나노 입자를 합성하였고, 다양한 분석장비들을 이용하여 이를 분석하는데 성공했다. 특히, NMR을 이용한 연구와 촉매 표면에서 일어나는 반응을 통해서 표면에 붙어 있는 비닐리덴 리간드를 확인할 있었다. 이렇게 만들어 진 로듐 나노 입자를 히드로포밀화 반응에 적용하였다. 우리는 촉매 반응을 통해 로듐 나노 입자가 훌륭한 활성도를 지닌다는 것과, 촉매를 분리하여 재사용 실험을 진행해 본 결과 다른 계면활성제나 리간드가 붙어 있는 나노 입자들에 비해 더 안정하다는 것을 확인할 수 있었다. 또한, 로듐 나노 입자의 표면에 붙은 비닐리덴 리간드의 변화를 줌으로써 나노 입자의 활성도에 차이를 줄 수 있다는 것 역시 확인할 수 있었다.

주요어 : 비닐리덴을 이용한 활성화; 로듐 나노 입자; 표면에서의 반응; 촉매 반응의 적용; 안정성

학 번 : 2012-23044